1996

Conveyor tracking using adept robot with vision guidance system

Chen-yu Wang

CONVEYOR TRACKING USING ADEPT® ROBOT WITH VISION GUIDANCE SYSTEM

BY

CHEN-YU WANG

A THESIS SUBMITTED
IN
PARTIAL FULFILLMENT
OF THE REQUIREMENTS FOR THE

MASTER OF SCIENCE

IN
MECHANICAL ENGINEERING

APPROVED BY:

PROFESSOR_____
DR. WAYNE W. WALTER, *THESIS ADVISOR*

PROFESSOR_____
DR. MICHAEL P. HENNESSEY

PROFESSOR_____
DR. ATHIMOOTTIL V. MATHEW

PROFESSOR_____
DR. CHARLES W. HAINES, *DEPARTMENT HEAD*

DEPARTMENT OF MECHANICAL ENGINEERING
COLLEGE OF ENGINEERING
ROCHESTER INSTITUTE OF TECHNOLOGY
OCTOBER 1996

PERMISSION FROM AUTHOR REQUIRED:

I, Chen-yu Wang, prefer to be contacted each time a request for reproduction of the thesis entitled CONVEYOR TRACKING USING ADEPT ROBOT WITH VISION GUIDANCE SYSTEM is made. I can be reached at the following address:

135 Mei-Chun Road Section #1
Taichung, Taiwan, R.O.C.
Tel/Fax: +886 (4) 321-3149

Date: October 14, 1996

Signature: _____
Wang, Chen-yu

Abstract

This thesis examines the integration of the robotic assembly workcell and the capability of the AdeptOne SCARA robot in performing both non-vision and vision based conveyor tracking. An experiment is set up for a Plastic Leadless Chip Carrier, or PLCC, chip and socket assembly operation. A PLCC chip is a square-shape integrated circuit that has its pins bent down around its perimeter to prevent damage to the pins during assembly and transportation. Binary image processing is employed by the vision system to recognize the random locations of incoming PLCC chips at the upstream location of the conveyor. When at least one PLCC chip is identified, the robot will acquire the chip using a special designed end effector and will wait until a printed circuit board passes the sensor at the downstream location of the conveyor. The robot will then insert the PLCC chip into the PLCC socket on the moving circuit board which is transported into the robot's work envelope by the conveyor. The circuit board is fixed on the conveyor belt. The entire operation is conducted without any interruption of the conveyor's motion. This thesis covers the design of the robot workcell and the end effector that accomplishes the assembly task and the results of non-vision and vision conveyor tracking during PLCC assembly using the Adept robot system.

Acknowledgment

I would like to take this opportunity to express my sincere gratitude to my parents who have long been the greatest support for my academic achievement. I also would like to thank my thesis advisor, Dr. Wayne Walter, for his guidance and encouragement and other committee members, Dr. Michael Hennessey and Dr. Athimoottil Mathew for their valuable comments throughout my efforts on this thesis.

PERMISSION FROM AUTHOR REQUIRED:

I, Chen-yu Wang, prefer to be contacted each time a request for reproduction of the thesis entitled CONVEYOR TRACKING USING ADEPT ROBOT WITH VISION GUIDANCE SYSTEM is made. I can be reached at the following address:

135 Mei-Chun Road Section #1
Taichung, Taiwan, R.O.C.
Tel/Fax: +886 (4) 321-3149

Date: October 14, 1996

Signature: _____
Wang, Chen-yu

Table of Contents

List of Figures

List of Tables

1. Introduction

In conventional manufacturing assembly lines, conveyors are widely used to move parts from one workstation to another. The conveyor belt has to stop at each workstation for a specific amount of time and wait until the assembly operation is completed before the conveyor can transport the parts to another workstation. The conveyor's stopping time adds up and lengthens the entire assembly process [1]. This delay causes a reduction in overall production efficiency, especially in automated assembly lines. In an effort to eliminate such a drawback, the concept of conveyor tracking is developed to ensure the consistent workflow of the assembly line by allowing assembly tasks to be performed while the conveyor is still moving. In a tracking conveyor system, the conveyor not only serves for the purpose of material handling but also acts synchronously with the automated process. Furthermore, a robotic tracking conveyor system is capable of feeding the continuous change of the parts' locations on the belt in real time back to the robot controller through the use of various sensors such as position, velocity, force, vision, and laser-guidance [2]. This thesis presents the use of the AdeptOne robot of the SCARA (Selective Compliance Assembly Robot Arm) type with a vision guidance system and a Dorner conveyor of the flat belt type [3] to demonstrate both non-vision and vision conveyor tracking in an automated assembly process.

The SCARA type robot was first developed by Professor Hiroshi Makino of Yamanashi University, with the support of thirteen Japanese companies. Because the

SCARA type robot was designed with the sizes of electric appliances in mind, it usually has the precision needed for the assembly of small components such as Integrated Circuits, or ICs, optical equipment parts and so on [4], [18]. Back in 1970's, General Motor Research Laboratory and Manufacturing Development Staff demonstrated the technical feasibility and potential usefulness of vision system on industrial parts [14]. In 1978, General Motors unveiled the Programmable Universal Machine for Assembly (PUMA) system that included conveyors, parts feeders, and robots small enough to work along-side humans. These small robots supplied by Unimation became known as the PUMAs [10]. Later in the early 1980's, Unimation developed a robot vision system which was named Univision I through the use of a Machine Intelligence Corporation binary vision system in conjunction with the Unimate PUMA robot. Its successor, Univision II, was further equipped with a two-pass seam tracking system which used a fiber optic light source to track the location of a weld [19]. The use of the vision information for tracking has also been reported in other research work [23], [26]. In addition, several researches have been conducted on the conveyor belt system coupled with a robot manipulator. Some significant work was done in the 1980's using a PUMA robot in conjunction with a conveyor tracking system. A common control method of the robot-conveyor belt systems uses the straight line trajectory planning to track the moving parts on a conveyor [25], [27]. The speed of the conveyor and the dynamics of the robot arm are also analyzed and formulated to improve the accuracy and reliability of the conveyor tracking system [24].

With an incremental encoder measuring the displacement of the conveyor, the AdeptOne robot can be programmed to be used in conjunction with non-vision and vision

conveyor systems. With a non-vision tracking conveyor, a sensor signals that a part has passed a known location. The robot controller tracks the progress of the belt and picks up the part when it comes into the robot working area. The parts must be in the same location with respect to the center line of the belt. With a vision equipped tracking conveyor, a fixed-mount camera takes regularly timed or strobed pictures of the belt and returns the location of parts it locates. Digital Input / Output, or I/O, can also be used to trigger the picture. These part locations are queued and picked up by the robot [5].

A growing number of studies have been conducted investigating various approaches to machine recognition of assembly parts [11], [15]. One of the approaches is based on the features of the object which are defined by a collection of patterns and the relations among them [9], such as used in the Univision I system [22]. A pattern is a visual clue to an object such as color, edge, texture, etc. Operations like edge detection, color distinction, and texture mapping are performed to extract features from an object's digitized image. Pattern matching is then realized by fuzzy reasoning from a database of features. Such technique is also known as pattern-based object recognition. Another common approach is model-based object recognition [12]. Instead of relying on a database of pre-defined geometric shapes and patterns of objects, models or geometric shapes of the recognizing object are first analyzed and memorized for the model matching operation. This is the technique the Adept vision system uses. The vision system accomplishes part recognition by using the descriptions of surface characteristics of a part and compares them to pre-trained prototype models [13], [20]. The percentage rate of "matching" decides the success rate of recognition.

The vision system equipped with the AdeptOne robot consists of a Charged Couple Device, or CCD, camera and a vision operating system software from Adept Technology called VisionWare [6]. The CCD camera digitizes the image it acquires in the form of a compositional array of pixel cells [7]. The acquired image is presented either in binary scale mode or gray scale mode. The binary scale image processing assigns each pixel either a 0 or 1 for black and white, whereas gray scale can assign gray values up to 16, 64, and 256. Several shades of gray are apparent because the system processes the variations in light intensity, or brightness, picked up by the camera. Brightness results from the way a surface reflects light, so digitizing brightness variations provide the robot controller with the information about the object's texture, depth, silhouette, and so on. Very much like the human visual system, binary scale and gray scale are passive. That is, they do not require interaction with an object in order to sense it. However, gray scale systems are limited because they require much more data processing than do binary system [4]. The implementation of the vision system allows the robot to acquire and assemble parts that are randomly placed and oriented.

The parts for assembly are Plastic Leadless Chip Carrier, or PLCC, chips and PLCC sockets. PLCC is the successor to the widely-used Dual-In-line Pin, or DIP, and Pin Grid Array, or PGA, packages for microprocessors. A PLCC chip has its pins bent down around its perimeter so it is much less subjected to pin damage [8], [17]. A PLCC socket is made of plastic instead of ceramics for cost-effective reasons [16]. Figure 1 shows the three types of most common IC chips in use today.

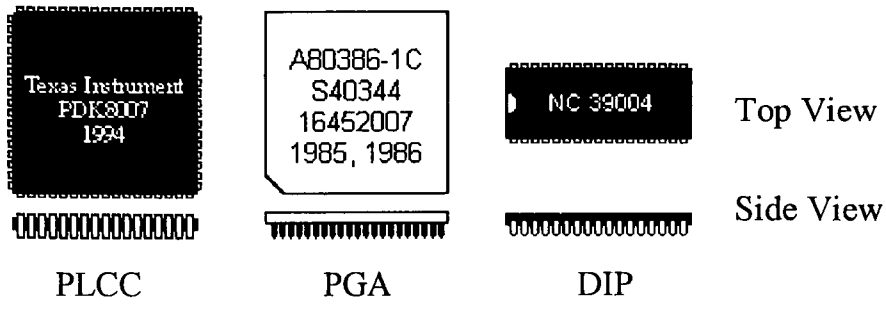

Figure 1: Various types of IC chips

During the assembly operation in this thesis, PLCC chips on a carrying tray are being transported to the upstream location of the conveyor where the fix-mounted camera will identify one chip's location and orientation and feed back the information for the robot to acquire the chip. Once the printed circuit board hits the sensor at downstream location of the conveyor, the robot will insert the acquired chip into the PLCC socket on the circuit board without the use of a vision system. When inserting the PLCC, the leads from the PLCC chip slide against the mating contacts inside the inner edge of the PLCC socket. The same assembly operation is then repeated for a second chip at another socket. The whole assembly takes place while all the parts are on a moving conveyor.

This thesis includes the pictures taken from the actual experiment and is organized in the following fashion. Section 2 describes the integration of the robotic workcell and section 3 lists the equipment setup and procedures for the robot workcell design. Section 4 details the design of the end effector to be used with the robot assembly operation. The results and discussion of the PLCC assembly using the conveyor tracking technique is

presented in Section 5 followed by comments on future implementations in Section 6. Finally, the conclusion is in Section 7.

2. Integration of the Robotic Workcell

In an effort to automate the process of the PLCC chip and socket assembly, the concept of system implementation is employed to integrate the robot system, vision guidance system, and the conveyor tracking system into a working assembly cell. This approach is based on the following advantages:

- The use of the robot system in an assembly task is highly efficient and cost effective.
- The vision system is able to identify the random positions and locations of parts based on their digitized images and to perform non-contact visual inspection of parts.
- The use of the conveyor tracking system can increase the overall assembly efficiency because it allows non-stop workflow of the assembly line.

A sequence of implementation is proposed to serve as the guideline throughout the work of the thesis. Figure 2 shows a chart listing the general layout of the sequence. In the analysis of the assembly parts, the parts are identified as the PLCC chips and sockets. Their physical dimensions, weight, fitting clearance, and surface properties are measured to be used as reference data for the design of the robotic workcell and the end effector. The design of the robot workcell is considered the most important step in the integration of the entire system. The arrangement of the hardware components such as the robot arm, the conveyor system, the vision system, and the optical sensors are all constrained to the robot's work envelope and the available space. Equipment such as the camera and encoder

will require calibration after they are installed. The detailed steps of the workcell design will be further discussed in Section 3. The end effector's intended functions and ease of manufacturing are taken into consideration during the design process. Mechanical debugging is performed after the fabrication of the end effector to ensure the prototype meets the specification and the feasibility requirement of the design. Section 4 of the thesis has a more detailed description on the design of the end effector.

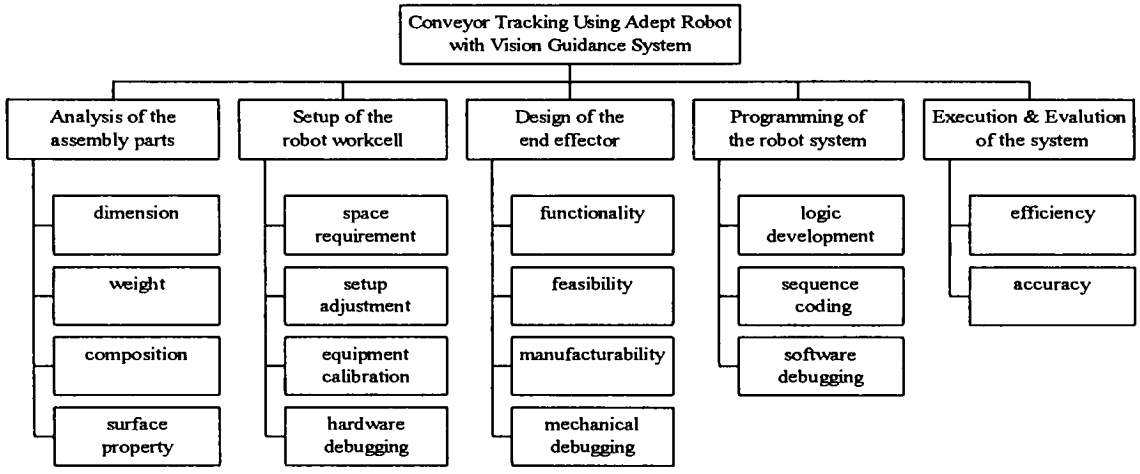

Figure 2: Sequence of implementation

After the completion of the hardware integration, software programming is required to control the system. The Adept robot system offers a user-friendly application software called Assembly Information Manager (AIM) based on the V/V^+ programming language. VisionWare is the AIM's software module used to control the camera and the vision operation. A sequence of tasks can be programmed using the MotionWare module to control the motion of the robot and other components in the workcell through the use of its digital Inputs and Outputs (I/Os). Software debugging is necessary to ensure the

smooth workflow of the workcell and the successful assembly of parts. Finally, the performance of the entire system is evaluated for its efficiency and accuracy, key factors to indicate whether the designed system has met the intended purpose.

3. Design of the Robot Workcell

3.1 Simulation of Continuous Conveyor

In most assembly lines, conveyors are used to move material over a fixed path. The path can be continuous or branched. Either way, they all run through or by specific workstations where assembly operations are performed. Because the laboratory is not equipped with the continuous conveyor as the one found in the industrial workplace, an attempt was made to simulate the movement of a continuous conveyor using a single conveyor belt, as shown below:

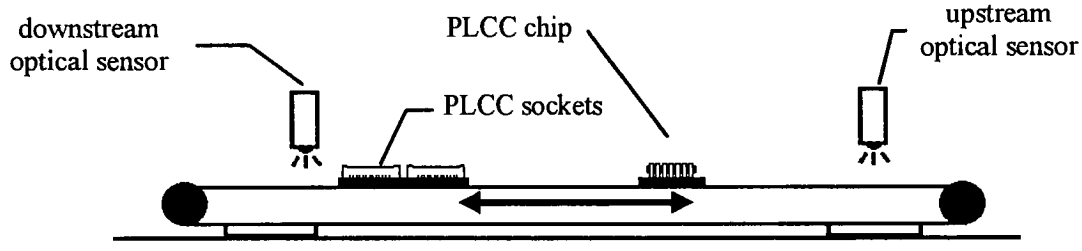

Figure 3: Simulation of continuous conveyor

Figure 3 shows the schematic of the simulation. Optical sensors are mounted both at the upstream and downstream of the conveyor belt where the parts (PLCC chips) and the assembly piece (PLCC sockets) are placed on the belt apart from each other at a distance. With the conveyor motor and both sensors hooked up to the robot controller's I/Os, a program sequence can be created to control the direction of travel of the conveyor belt. The conveyor belt is programmed to reverse its direction of travel whenever either of the upstream or downstream sensors is triggered by the assembly piece or the parts. The

conveyor will move back and forth until the robot control turns off the belt when the assembly operation is completed. Thus, the behavior of the conveyor movement simulates the non-stop condition of a continuous conveyor.

3.2 Selection of Sensors

In order to detect parts' presence at the upstream and downstream positions of the conveyor, optical sensors are mounted at each respective location. To be more specific, the optical sensors used are the infrared type which are capable of non-contact and non-destructive detection of objects. The infrared light beam the sensor emits is an ideal choice of triggering source because of its quick response time. Unlike an Eddy Current sensor or a magnetic-type sensor, the infrared beam does not damage the sensitive circuitry of the IC chips. The non-contact detection also ensures that the part is not displaced in any way when it is detected by the sensor. This is a very important factor in the accuracy of conveyor tracking. Figure A- 4 in Appendix A3 shows the diagram of the infrared optical sensor with wiring information.

3.3 Position of the Camera

When programming the AdeptOne robot to perform conveyor tracking with vision option, its calibration software only allows the camera to be mounted at a fixed position rather than on the robot arm. If the camera is mounted on the robot arm for conveyor tracking assembly, the robot arm would be performing two tasks simultaneously: move the camera with respect to the moving conveyor to take the picture of the incoming part and, secondly, track the parts for assembly. It means that all the coordinate transformations

(see Figure 4) between the camera-to-robot, camera-to-conveyor, and robot-to-conveyor need to be computed at once. This requires a considerable amount of processing power which the Adept's Compact Controller lacks. The longer processing time gives less time for the robot to successfully track and assemble the parts before they move out of the robot's work envelope. Thus, configuring the camera to be mounted on the robot arm for conveyor tracking is not a feasible option in setting up the camera and the robot. Instead, the camera is mounted at a stationary position upstream of the conveyor.

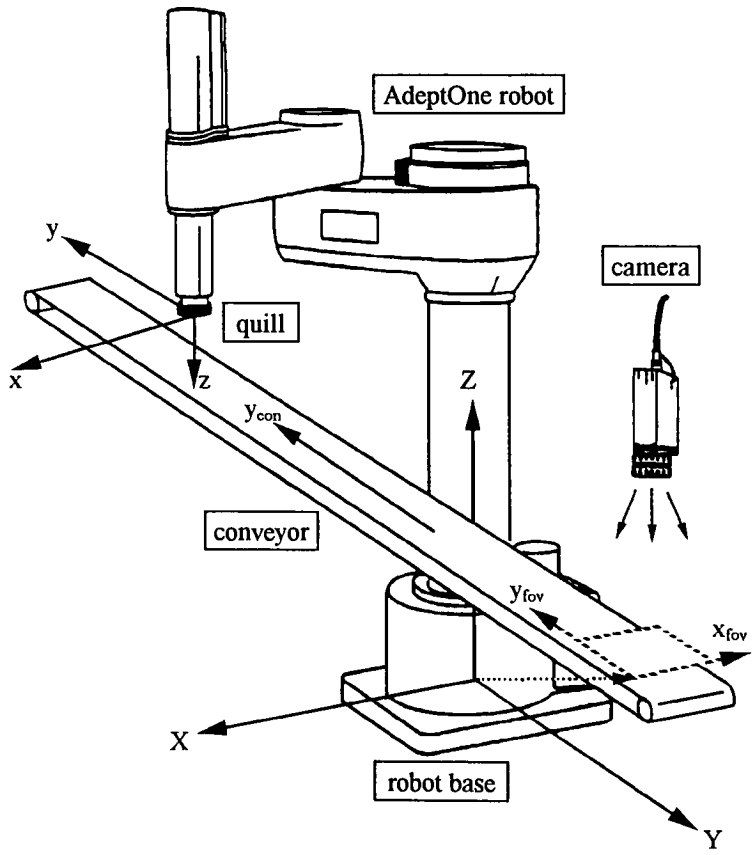

Figure 4: Camera and conveyor locations with respect to the robot

When setting up the camera for vision operation, it is preferable to mount the camera at a stationary location as close to the robot's work envelope as possible and not to interfere or limit the robot arm's movement too much. Because the accuracy of conveyor tracking with vision relies on the coordinate transformation between the camera's picture-taking location and the robot's work envelope (See Figure 4), the longer the part has to travel from the camera's location into the robot's reachable work space the greater the error will result from the encoder counts. Since the parts are placed on the surface of the conveyor belt and vision recognition is performed on the top surface of the parts, the camera needs to be placed facing downwards. A camera fixture was built to hold the camera right above the upstream sensor at a height that the camera's 25 *mm* lens was able to cover a complete visible section of the conveyor belt. The reason the picture-taking location is set at the top of the upstream sensor is that the upstream sensor is also used to trigger the camera to take a picture when parts are presented at this location. Once the camera and the conveyor are placed in fixed locations, it is necessary to calibrate the camera using the robot controller's calibration program to set up the camera's properties and to establish the relationship between the camera and conveyor locations with respect to the robot's world coordinate. Figure 5 shows a picture of the actual mounting location of the CCD camera.

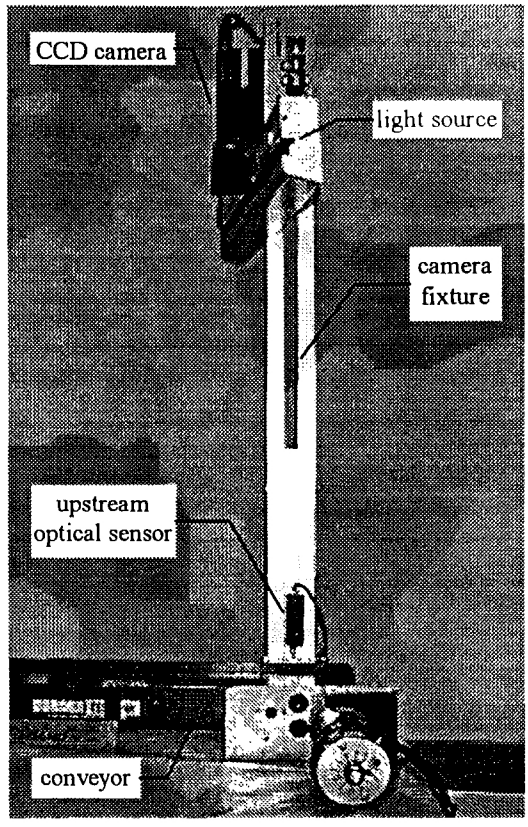

Figure 5: Picture of the camera's mounting location

3.4 Parts for Assembly

The parts for assembly are identified as 68-pin PLCC chips. They are fed into robot's work envelope on a carrying tray. In order to minimize the vibration resulting from the conveyor's motion, the tray is made of aluminum which is considerably heavier and more rigid than the conventional plastic tray. The carrying tray is a piece of square plate which can accommodate up to four 68-pin PLCC chips at once. Because vision recognition is used for part acquisition, the PLCC chips can be placed at random orientations on the tray with the condition that their top surfaces need to lay flat and the top surface would automatically face upward for vision recognition. Figure 6 shows the

top view of a 68-pin PLCC chip. There are two fiscal marks and a chamfer cut on the upper left corner of the square chip. These are the surface characteristics used by the vision operation to identify the chip's orientation.

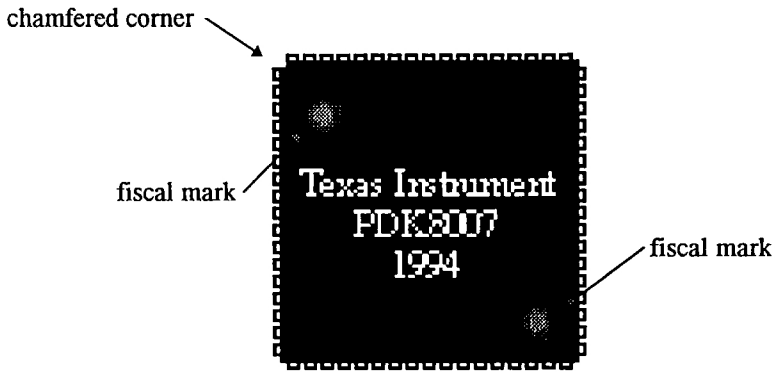

Figure 6: Schematic of a 68-pin plastic leadless chip

The other part, or "pallet" for assembly is a circuit board with 68-pin PLCC sockets. The circuit board is fixed to a piece of aluminum plate to ensure stability while it is being moved on the conveyor.

Figure 7 shows a picture of the circuit board with different sizes of PLCC sockets. Because the PLCC sockets' locations and orientations are always fixed with respect to the circuit board, as long as the circuit board is locked at a fixed position relative to the conveyor belt, no camera is needed to find the sockets' locations. Instead, the downstream sensor will signal the robot the whereabouts of the PLCC sockets once the circuit board hits the downstream sensor. The picture representation of the setup at the downstream location of the conveyor is shown in Figure 8.

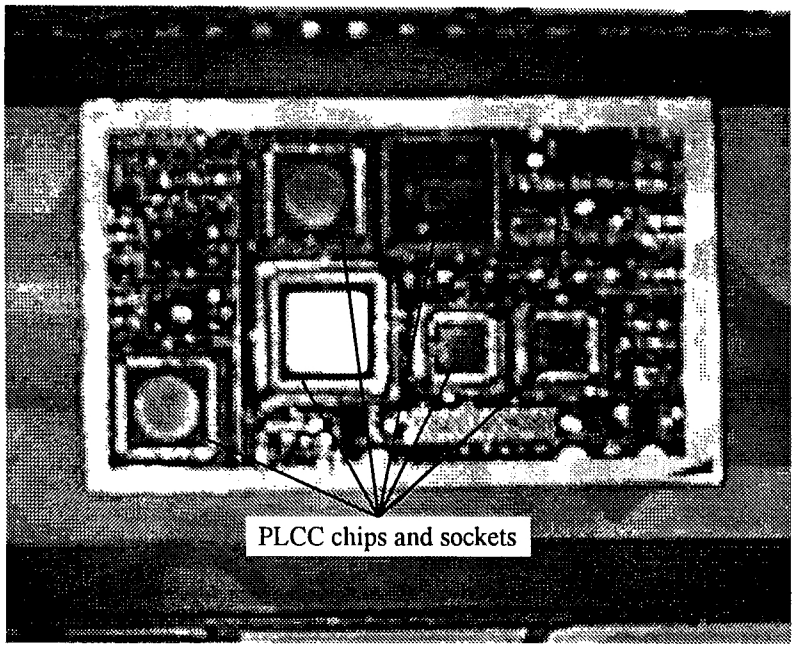

Figure 7: Picture of a circuit board with PLCC sockets

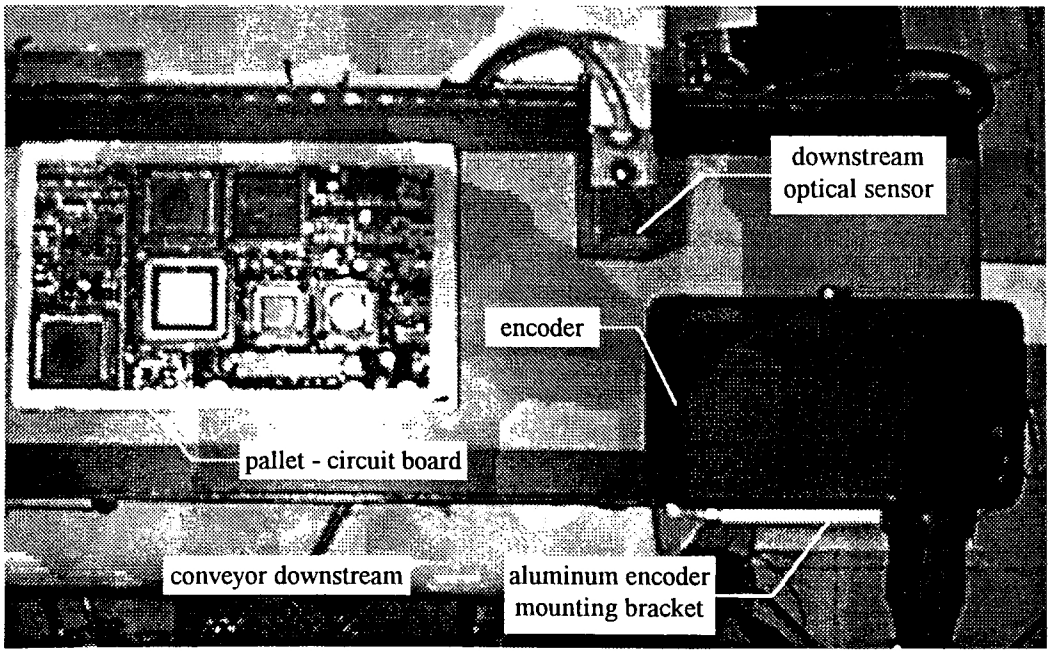

Figure 8: Encoder's mounting location

3.5 Encoder Mounting

The encoder is used by the robot controller to keep track of the movement of the conveyor belt. Even though it is preferable to mount the encoder on the bottom of the conveyor so that the presence of the encoder does not interfere with the parts that are being transported on the belt, the design of the conveyor used does not allow such method of encoder attachment. After visual examination of the conveyor, it was determined that the area between the downstream end of the conveyor and the downstream sensor is the best alternative to place the encoder. Because the conveyor would reverse its direction of travel if a part is detected by the downstream sensor, no part is supposed to be present in this area. In addition to that, this area is also outside the robot's work envelope so the encoder will not interfere with the part's transportation and the robot's movement if it is mounted within this area. The black box shown at lower-right in Figure 8 is the actual mounting location of the encoder. The shinny white piece below the encoder is the aluminum mounting bracket.

3.6 Light Source

The CCD camera used for vision recognition is very sensitive to its surrounding lighting condition. A good source of lighting can ensure a higher image quality, hence, it increases the success rate of image recognition. The fluorescent tube was chosen to be the light source for the camera. Because the fluorescent tube is of the diffuse lighting type which illuminates a surface with light that strikes the surface from many different angles,

shadows and reflection can therefore be minimized. Figure 9 shows how diffuse lighting illuminates a working surface.

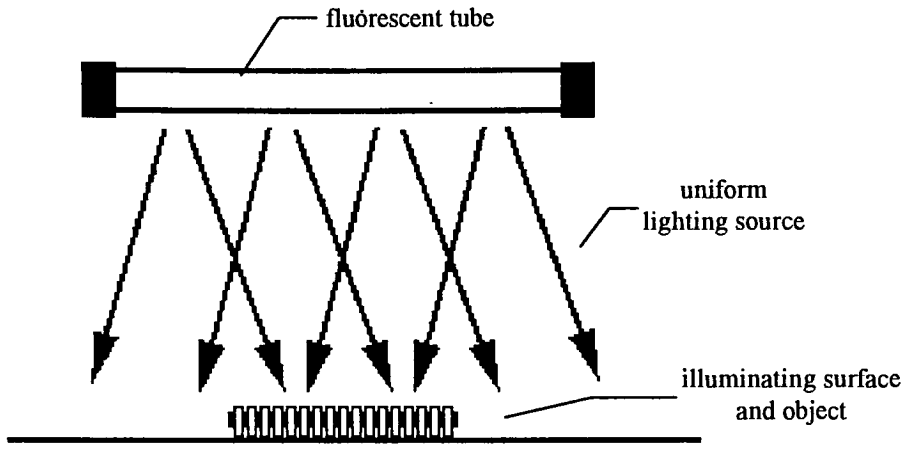

Figure 9: Diffuse lighting using a fluorescent tube

The fluorescent tube is mounted just below the camera's mounting position to provide direct diffuse lighting from the top onto the surface of the conveyor. Figure 5 shows where the fluorescent is mounted on camera's fixture.

3.7 Control of Digital I/Os

After the setup of all the peripheral equipment is completed, it is necessary to connect it to the robot controller's digital I/Os so the robot will have control over the equipment. Table 1 shows a complete list of all the digital I/O signals that are assigned and controlled for this experiment. The soft signals listed do not have physical connections to the digital I/O ports. They are used as internal tag signals that are software controllable.

Table 1: List of I/Os

	Signal	On	Off
Input Signals	**1001**	presence of part at upstream	absence of part at upstream
	1002	presence of part at downstream	absence of part at downstream
	1003	== NOT USED ==	
	1004	== NOT USED ==	
Output Signals	**0009**	conveyor power on	conveyor power off
	0010	upstream-to-downstream direction of travel	downstream-to-upstream direction of travel
	0011	end effector air solenoid on	end effector air solenoid off
	0012	3-port solenoid air on	3-port solenoid vacuum on
Soft Signals	**2001**	conveyor ready for use	conveyor not ready for use
	2030	tool changer air solenoid on	tool changer air solenoid off
	2031	vacuum tool air solenoid on	vacuum tool air solenoid off
	2041	chip #1 successfully recognized tag	chip #1 unsuccessfully recognized tag
	2042	chip #2 successfully recognized tag	chip #2 unsuccessfully recognized tag

The 3-port solenoid listed in Table 1 is a control device to switch between air and vacuum on a single air line. Figure 10 shows a schematic of the physical air line connection of the 3-port solenoid. The solenoid has two ports of input: one for compressed air and the other one for vacuum and a single port for output. The output port is connected to the end effector's pneumatic cylinders via an air line. The "air/vacuum" behavior of the air line can cause the single-acting pneumatic cylinder to function like a double-acting one. The double-acing pneumatic cylinder has the advantage of fast stroke reaction which is very critical when the PLCC chip is being inserted into the PLCC socket while the socket is in motion. Figure 11 shows the picture of the vacuum pump that is used in this experiment.

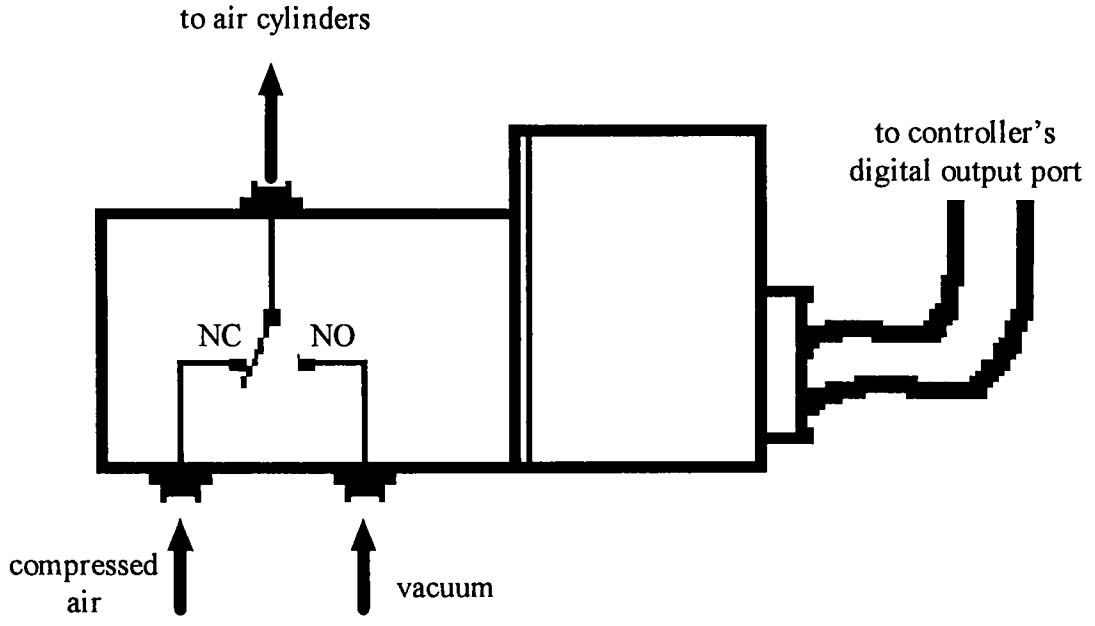

Figure 10: Schematic of the 3-port solenoid connection

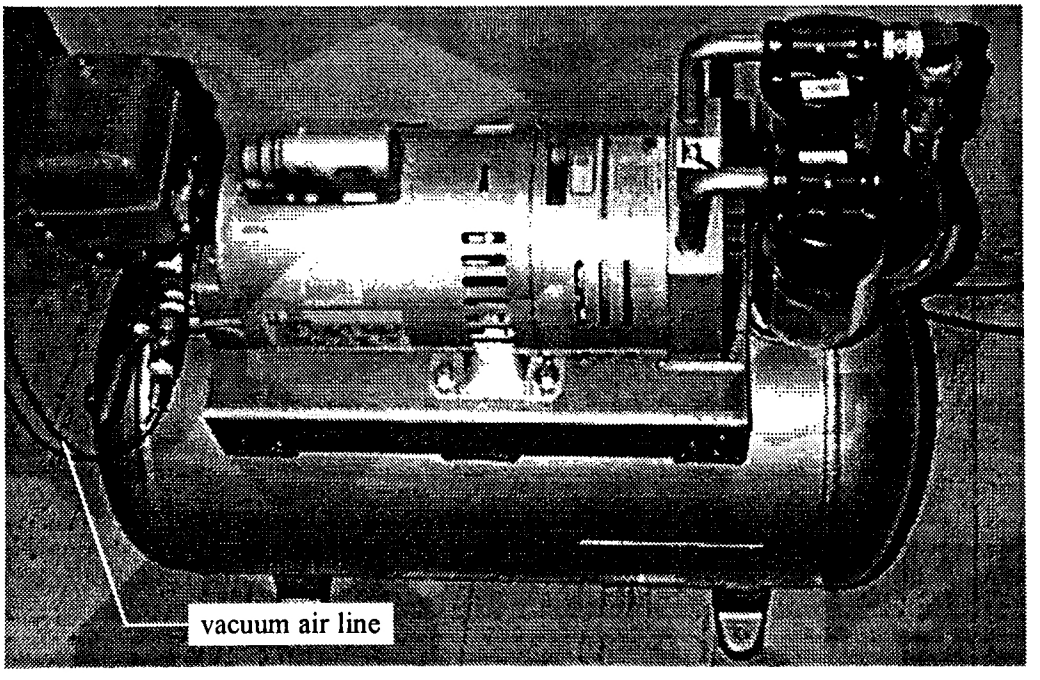

Figure 11: Picture of the vacuum pump

During the experimental stage of the assembly, the conveyor was tested for its moving speed and stability. It was decided to replace the belt's single-phase AC motor with a 90 VDC speed-controllable gearmotor[1]. The motor's electrical wires were modified and a polarity reversing relay was designed to connect the motor to the robot's digital I/Os so the motor's power and direction of travel could be fully controlled by the robot controller. Figure 12 shows the diagram of the relay circuitry. Relay 2 and 3 are wired to the same on/off digital signal so both relays are either at NO (Normally Open) or NC (Normally Closed) position. When they are closed, the current from the speed controller will pass through relay 1 and 2 to motor's A1 terminal and the ground will pass relay 3 to motor's A2 terminal. On the contrary, A1 terminal will be connected to the ground and A2 to the current when both relay 2 and 3 are open. Relay 1 simply acts as an power on/off switch for either of the current or the ground signal.

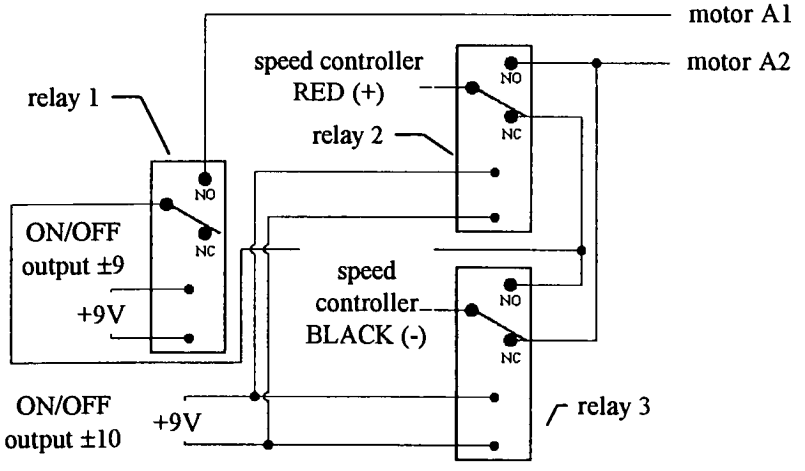

Figure 12: Diagram of the polarity reversing relay

[1] Technical data of the gearmotor is in Appendix A-5.

Figure 13 shows the picture of how the DC gearmotor is connected to the conveyor using a coupling to accommodate the misalignment of the two shafts.

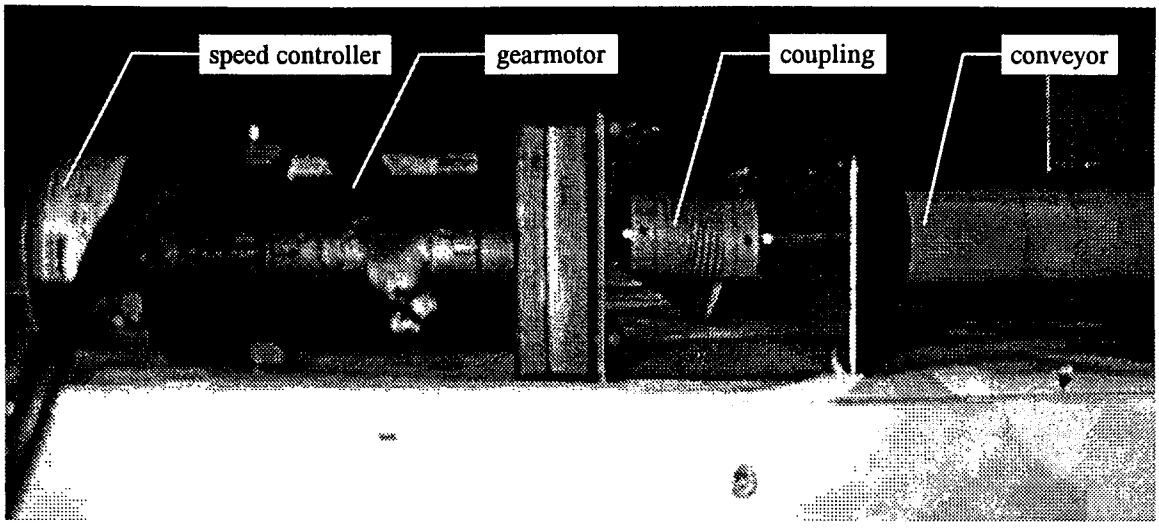

Figure 13: Picture of conveyor DC gearmotor

3.8 Final Setup and Programming

After securing each piece of equipment in place, their locations should remain unchanged. Otherwise, camera-to-robot and robot-to-conveyor calibrations will need to be repeated if any of the equipment is adjusted in any way. Figure 14 shows a pictorial view of the coordinate transformation between the robot and the camera. The robot base is defined as the world coordinate. The square dashed box underneath the camera represents the Field of View, or FOV, of the camera which is attached to the vision coordinate system. While the coordinate relationship between the robot base and the center of the robot quill has been established during the initial startup of the robot arm, the

camera-to-robot coordinate transformation can be computed using the calibration software through the movement of the robot quill with a calibration tool attached to it and a calibration disc placed within the FOV of the camera.

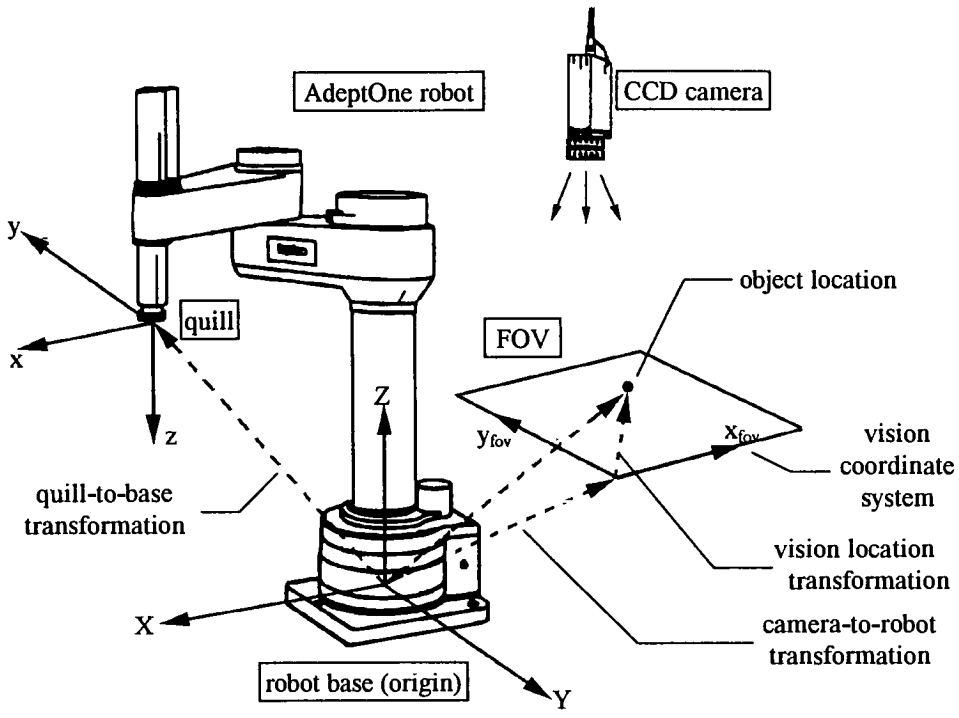

Figure 14: Camera-to-robot coordinates transformation

The robot-to-camera calibration establishes the coordinate transformation from the robot base (world coordinate) to the lower left corner of the FOV of the camera (origin of the vision coordinate system). Any object viewed under the FOV is related to the vision coordinate system. A tool offset is simply an additional coordinate transformation with respect to the quill coordinate system. The same principle applies to the robot-to-conveyor calibration except that the conveyor coordinate system is a moving one which is updated in real time through the use of the encoder (see Figure 4 for conveyor coordinate

definition). Figure 15 shows a picture[1] of the complete design of the robot workcell. Appendix C lists the important procedures for programming the robot and the vision system.

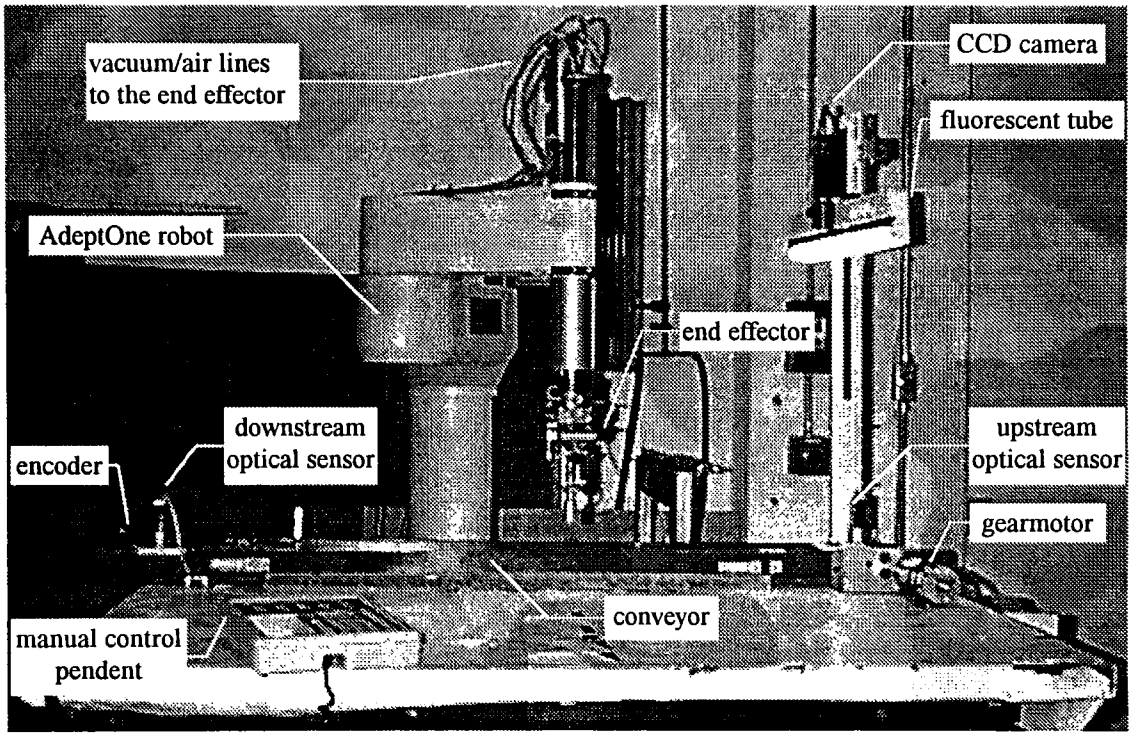

Figure 15: Picture of the robot workcell

[1] The robot controller, digital I/Os, and the solenoids are not in the picture.

4. Design of the End Effector

4.1 Design Criteria

A special robot end effector is designed to accommodate the delicate nature of the PLCC chip assembly process. Several design conditions are taken into consideration in the design of the end effector. Because the assembly process involves pick-and-place movement, it is preferred that both the "pick" and "place" tasks can be accomplished with the same end effector. The first problem in the pick-and-place process is that the PLCC chips are very light in weight and they require more than 10 lb. vertical force to be inserted into the PLCC sockets. This poses a great difference between the required lifting force and insertion force. Since the entire assembly takes place on the moving conveyor, quick response of the end effector becomes an important factor for successful chip acquisition and insertion. A convenient feature will be to make the end effector compatible with the existing Schunk Tool Changer adapter so that the end effector can be a detachable tool to the end of the robot quill.

4.2 IC Chip Insertion Force Measurement

In order to determine the force required to insert the IC chips into the PLCC socket, a quantitative approach is taken. A linear force gauge is used to measure the vertical insertion force of each chip. The force gauge is first calibrated and reset to zero. The contacting tip of the force gauge is a small piece of aluminum disk, roughly the same size as the head of the end effector. The PLCC chip is gently placed right on the top of the

PLCC socket before any vertical force is applied. While holding the force gauge vertically against the surface of the chip, a downward force is gradually applied until the complete insertion of the chip in the socket is observed. The dial indicator on the force gauge shows the maximum force that is ever applied during the insertion process. The same procedure is repeated several times to ensure the result's repeatability. The following is a table of the results:

Table 2: Insertion force of the PLCC chips

Trial(s)	Vertical Insertion Force, *lb.*
1	11.25
2	12.75
3	11.25
4	12.50
5	10.00
6	10.25
7	11.75
8	11.25
9	11.50
10	13.25

Maximum Force
13.25 lb.

Minimum Force
10.00 lb.

Average Force
11.575 lb.

4.3 Pneumatic Cylinder Force Requirement

From the measurement of the force required to complete the insertion, a maximum of 13.25 *lb.* needs to be produced by the end effector. Since the insertion process will have to occur while the PLCC sockets are in motion, a motor-driven crank mechanism that is capable of supplying continuous force will take too much time to reach the desired force. Therefore, pneumatic cylinders become a feasible choice to provide the source of force. Even though pneumatic cylinders do not have good controllability over their exerted force

and traveling distance, they are fast in response, low-cost, simple to use, and behave with a certain degree of compliance due to the compressible nature of the supply air.

To minimize the size of the end effector, it is desirable to have a pneumatic cylinder that is small in size and provides just enough force as required. After looking through several pneumatic cylinder vendor catalogs, the Bimba Manufacturing Company was found to carry a wide range of selections in pneumatic cylinders. It was further determined that the Bimba single-acting stainless air cylinder with ½" stroke length and 7/16" bore is the ideal choice of a driving mechanism for the end effector. To calculate the force F_{cyl} exerted by the pneumatic cylinder simply multiply the air pressure P_{air} and the cross-sectional area of the piston A_{cyl}, as follows:

$$F_{cyl} = P_{air} \cdot A_{cyl} \tag{1}$$

or

$$F_{cyl} = P_{air} \frac{\pi D_{cyl}^{\ 2}}{4} = 80 psi \frac{\pi \left(\frac{7}{16} in\right)^2}{4} = 12.026\ lbf \tag{2}$$

where the area of the cylinder has been expressed in terms of its diameter D_{cyl}.

From the force calculated, using two of the same pneumatic cylinders will provide a total exerting force of 24.052 *lb.* if these two cylinders are mounted in parallel. Due to the fact that there is small contact friction between the pistons and the cylinder bodies and the cylinders are single-acting with spring return mechanisms, the actual force exerted is slightly less than the calculated value. It was therefore decided that two cylinders would be necessary.

4.4 Final Design

The final design of the end effector consists of three distinctive parts: the driving mechanism, the insertion head, and the vacuum tool. Figure 16 shows the schematic of the end effector.

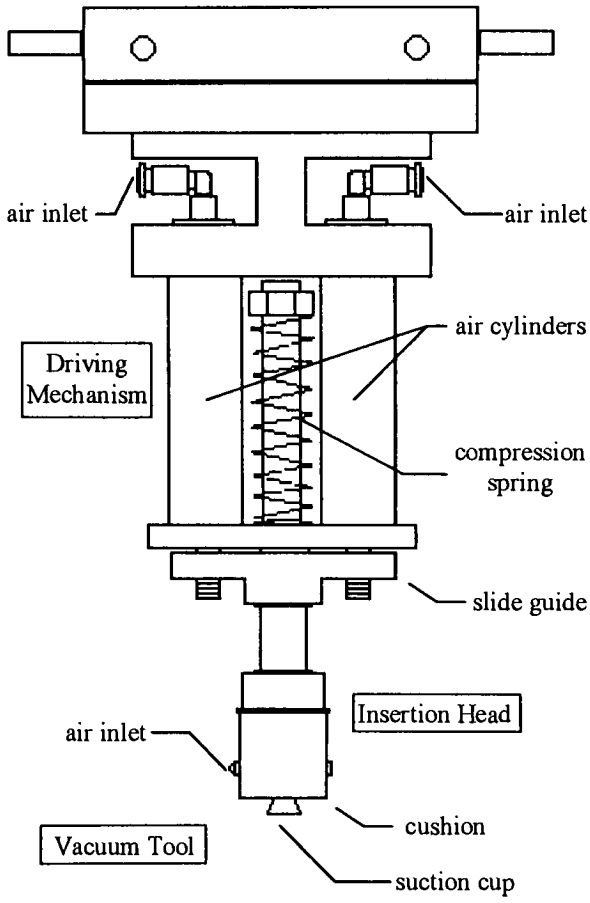

Figure 16: Schematic of the end effector

The driving mechanism consists of two Bimba[1] pneumatic cylinders that are mounted in parallel. When air pressure is supplied, the pneumatic cylinders are able to

[1] Bimba air cylinder model 01-1/2.

extend a stroke length of 0.5 *in.* The compression spring on the sliding rod was used to aid the pneumatic single-acting cylinders to reduce the time required to retract the piston rod once the air pressure is released from the cylinders.

Consider a free-body diagram of the slide guide of the end effector shown in Figure 17 ,where F_{cyl} is the force exerted by the cylinder, F_{spr} is the force exerted by the spring, F_{fri} is the frictional force resulting from the sliding contact and W_{tot} is the total weight,

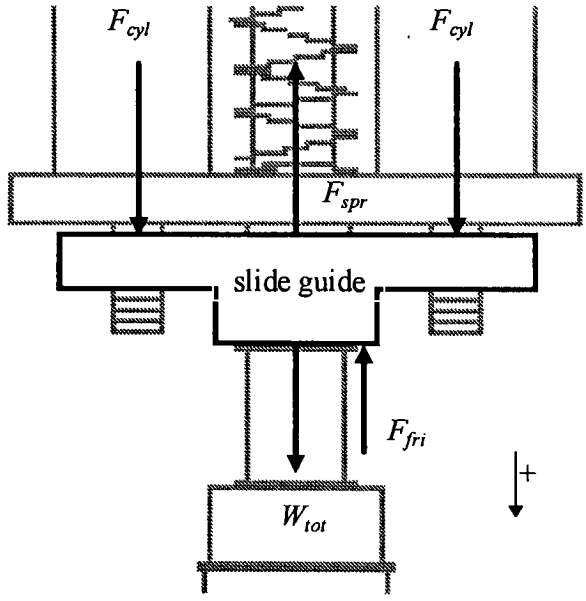

Figure 17: FBD of the slide guide of the end effector

the total force produced by the slide guide, F_{tot}, is simply the summation of the all the forces shown in the free-body diagram. From equation (2), F_{cyl} was found to be 12.026 *lb*. F_{spr} is the product of the spring constant and the stroke length of the slide guide. F_{spr} was calculated to be - 10 *lb*. W_{tot} is approximately the total weight of the slide guide, insertion head, and the suction cup. It was measured to be 0.2 *lb*. Both the sliding rod and the slide

guide are surfaced-polished to reduce the contact friction when sliding. It is assumed that 5% of the total output force will be lost due to the friction. Therefore, the total output force is

$$F_{tot} = 2F_{cyl} + F_{spr} + W_{tot} = 14.252\ lb \quad (3)$$

$$F_{act} = 95\%F_{tot} = 13.54lb \quad (4)$$

The equations above determine the actual total force output to be 13.54 *lb.*, which is slightly larger than the maximum required insertion force of 13.25 *lb.*[1] The calculated valued confirms that the design of the driving mechanism is feasible to accomplish the insertion task.

The insertion head is a piece of hollow cylinder made of aluminum. It is connected to a sliding rod which is controlled by the driving mechanism. The diameter of the head is machined close to the surface size of the 68-pin PLCC chip so when the head is used to push the chip into the PLCC socket, it provides a uniform distributed force on the surface of the chip. A separate piece of double-sided tape is attached to the end of the insertion head to serve as a cushion between the contact surface of the head and the IC chip. Figure 18 shows how the insertion head will complete the insertion process.

[1] Maximum insertion force measurement was explained in section 4.2.

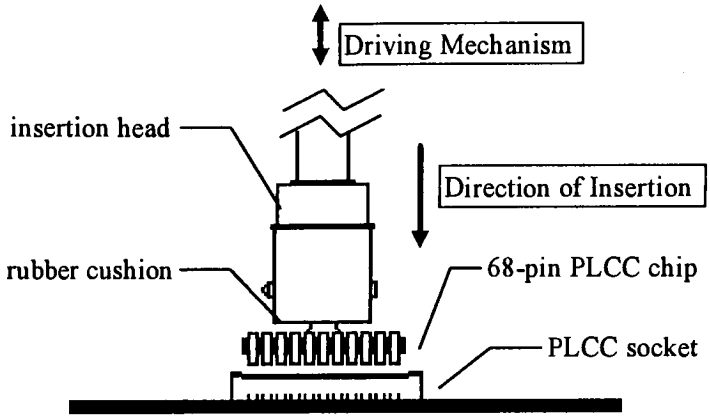

Figure 18: Chip insertion process using the insertion head[1]

The vacuum tool is housed partially inside the hollow space of the insertion cylinder. The vacuum tool is the Sommer Automatic[2] spring-loaded suction cup with a build-in vacuum generator. The schematic of the vacuum tool in Figure 19 shows how the build-in vacuum generator works based on the Bernoulli principle. When high speed air passes through the small nozzle, vacuum is created in the suction cup. Even though such vacuum is not able to provide a very high suction force, for the size and weight of a 68-pin PLCC chip, the lifting force produced by the vacuum tool is sufficient. The spring-loaded mechanism of the vacuum tool provides a small degree of vertical compliance to accommodate work pieces of varying heights. The complete assembly drawing of the end effector is included in the Appendix B-1 and the detailed drawings of the machined parts are included in Appendix B2 to B-8.

[1] The complete dimensional drawings of the insertion head are in Appendix B-7 and B-8.
[2] Sommer Automatic model FCV+NS8.

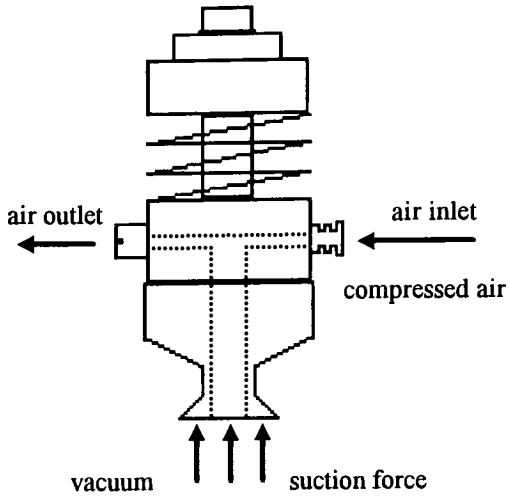

Figure 19: Sommer Automatic suction cup with vacuum generator

Figure 20 shows a picture of the designed end effector that is attached to the Schunk Tool Changer adapter at the end of robot quill. There are two air lines running to the end effector. One is connected to the cylinders of the driving mechanism and the other one is to the vacuum generator of the vacuum tool. During the process of mechanical debugging, several minor modifications were made to enhance the rigidity of the end effector's structure and to increase its degree of concentricity with respect to the center of the robot quill. The end effector was tested extensively for chip acquisition and insertion. Several successful attempts proved that the end effector was capable of completing the required task.

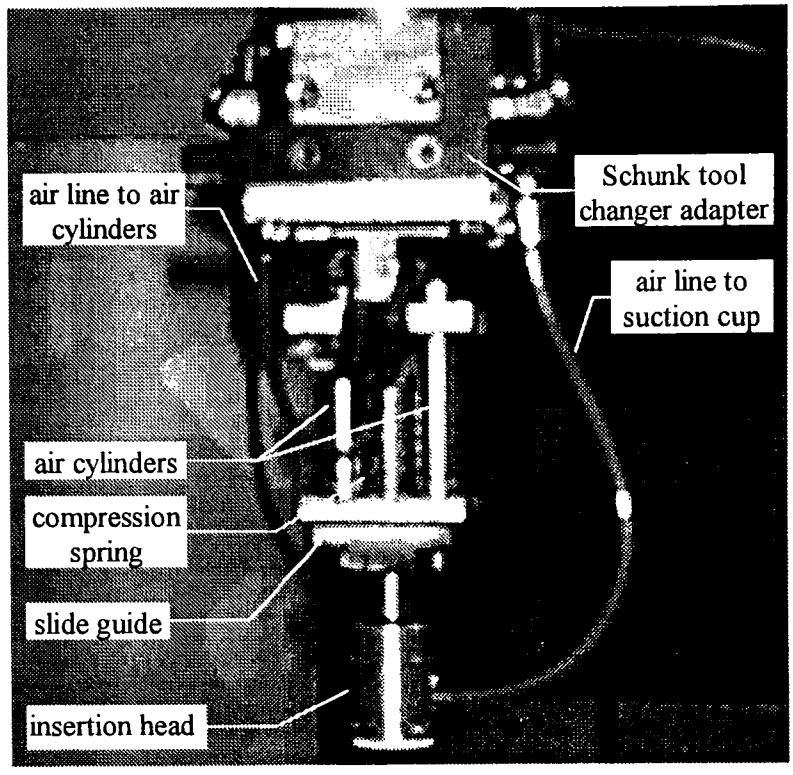

Figure 20: Picture of the end effector

5. Results and Discussion

5.1 Conveyor Tracking

The external incremental encoder plays an important role in the accuracy of the conveyor tracking system. The encoder makes use of a rotary mechanism to count the distance the conveyor has traveled, that is, a rotary disc is in contact with the surface of the conveyor belt all the time. The surface of the rotary disc is encoded with binary codes so the optical sensor inside the encoder is able to "read" the direction and distance of travel while the disc is being rotated by the conveyor belt.

In an assembly operation, conveyor calibration determines the accuracy of the conveyor tracking system. During the calibration, the robot controller computes and establishes the transformation relationship between the robot's world coordinate and the conveyor's "moving" coordinate. The conveyor "moving" coordinate becomes a special type of reference frame relative to the robot's location. The encoder updates the information of the constantly-changed reference frame to the robot controller in real time so the robot is able to pinpoint any location on the moving conveyor. Table 3 shows the robot-to-conveyor transformation as a result of the conveyor calibration. These values were determined within the robot control software during the calibration.

Table 3: Robot-to-conveyor transformation

	Lateral Direction (y-axis), *mm*
Maximum error for points used	0.009
Minimum error for points used	0.002
Average error for points used	0.006

The conveyor calibration shows an average error of ± 0.006 *mm* and the maximum error of ± 0.009 *mm* in the lateral direction, or the y-axis (see Figure 4 for coordinate definition). Although such small values indicate that the conveyor tracking system is rather precise in terms of accuracy, any value smaller than 0.01 *mm* is a quantity difficult to measure unless in a controlled environment. Therefore, it is assumed that these values are the result of mathematical interpolation within the software and the significant figure is up to the second decimal digit. The accuracy of the conveyor tracking is therefore within ± 0.01 *mm*.

There exist small gaps between the width of the belt and the conveyor platform. These two gaps are designed as a tolerance for the smooth movement of the belt. These gaps may cause the belt to move sideways slightly when it is moving and result in an inaccuracy in the x-axis direction of the conveyor. The inaccuracy was measured as ± 0.076 *mm* in the x-direction. Figure 21 shows a pictorial view of the described scenario.

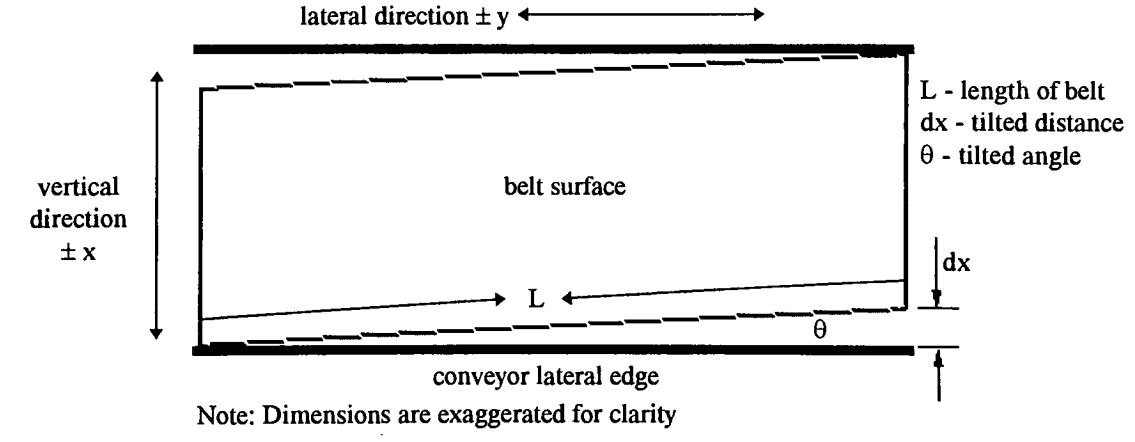

Figure 21: Conveyor tolerance

To calculate the rotational angle resulting from the inaccuracy:

$$\theta = \sin^{-1}\frac{dx}{L} = \sin^{-1}\frac{2 \times 0.076mm}{1524mm} \cong 0.01^{\circ} \qquad (5)$$

At the downstream end of the conveyor, no camera is used to identify the PLCC sockets on the circuit board when they pass this position. Because the encoder can only monitor the distance change in the y direction (see Figure 21), the robot controller will not be able to track the exact locations of the PLCC sockets if they are displaced in the x direction. Therefore, their locations should always be fixed with respect to the lateral edge of the conveyor. Once the circuit board triggers the downstream sensor, the robot will know the exact locations of the PLCC sockets as they move along on the conveyor. Figure 22 shows a pictorial view of the situation. In an industrial environment, the conveyor will be equipped with some kind of locking devices to insure the circuit board is secured on the conveyor.

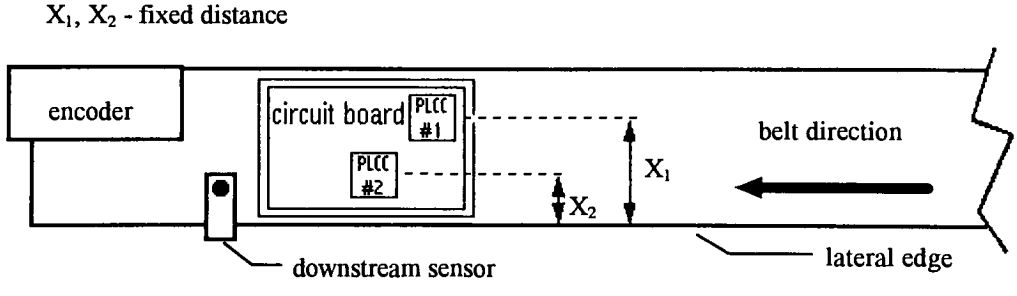

Figure 22: Locations of the PLCCs with respect to the conveyor

Another source of error that might contribute to the tracking conveyor accuracy is the vibration resulting from the conveyor driving motor. Any vibration and motion of the conveyor belt that the encoder's spring-loaded rotary disc can not compensate for will

result in an inaccurate encoder reading. This happened to be the case when the encoder was first mounted onto the conveyor using a piece of sheet metal. Due to the mechanical property of the sheet metal, this mounting piece was not able to sustain the constant vibration from the conveyor's motor and caused the encoder to vibrate along with the conveyor belt. The result was a ± 1.2 *mm* calibration error which was unacceptable for the PLCC chip assembly. The mounting piece was later replaced with a more rigid aluminum plate. Therefore, the mounting bracket ought to be stiff enough so the vibration transmitted through the bracket to the encoder would be kept at its minimum. Once the encoder was secured in position, robot-to-conveyor calibration should be performed to test the reliability of encoder's accuracy.

Over time, the rotary disc in the encoder can accumulate dirt or other objects and it will affect the encoder counts. Scheduled maintenance is required to ensure consistent performance of the encoder.

5.2 Vision Operation

The accuracy of the vision operation at the upstream location of the conveyor relies primarily on the camera-to-robot calibration performed after the complete setup of the robot and the conveyor. During the camera-to-robot calibration, the robot controller computes and establishes the transformation relationship between the robot world coordinate and the camera's mounting location. The result of the calibration is shown in Table 4. The result was automatically computed within the controller's software. The pixel's maximum error indicates the smallest pixel the camera is able to distinguish. The

reason the pixel number is less than 1 is that sub-pixel level processing is used. Mathematical interpolation is implemented in the process to obtain the highest accuracy.

Table 4: Calibration result of the camera-to-robot transformation

	Basic Calibration			Perspective Calibration		
unit measurement	***mm***	***in.***	**pixel**	***mm***	***in.***	**pixel**
Maximum Error	0.108	0.0041	0.4	0.057	0.0022	0.2
Average Error	0.103	0.0041	0.4	0.039	0.0015	0.2
Standard Deviation	0.119	0.0047	0.5	0.046	0.0018	0.2

The values of the basic calibration is the result of the initial camera-to-robot calibration. After gathering sufficient reference data during the calibration, the robot controller was able to determine the best-fit robot-to-camera transformation which simply established the relationship between the camera's mounting position and robot's location with respect to the conveyor. During the process of the calibration, the robot controller was able to determine the level of "flatness" of the conveyor belt's surface. Because the way the conveyor was supported did not allow the surface of the belt to be perfectly perpendicular to the camera's facing direction, it was suggested by the calibration program to use the perspective calibration to improve the accuracy. By taking the tilted angle of the belt surface into account, the calibration program computed the perspective compensation in an effort to minimize the inaccuracy resulting from the tilted surface. Table 4 also lists the result of the perspective calibration. It is evident that there was about 50% increase in accuracy improvement over the result of the basic calibration.

From the result of the camera-to-robot calibration, the vision system is capable of recognizing the image under the Field of View, or FOV, to an accuracy within $\pm$ 0.057

mm. The actual size of the FOV was measured to be 123.2 *mm* x 122.7 *mm*. The CCD camera used has a resolution of 501 x 485 pixel array. So, to calculate the translation and rotation error:

$$R_w = \frac{w_{FOV}}{w_{pixels}} = \frac{123.2mm}{501pixel} = 0.246\frac{mm}{pixel} \cong 0.2\frac{mm}{pixel} \quad (6)$$

$$R_h = \frac{H_{FOV}}{H_{pixel}} = \frac{122.7mm}{485pixel} = 0.253\frac{mm}{pixel} \cong 0.3\frac{mm}{pixel} \quad (7)$$

where R_w is the vertical resolution (x-axis), R_h is the horizontal resolution (y-axis), W_{FOV} and H_{FOV} are the vertical and horizontal sizes of the camera's field of view respectively, and W_{pixel} and H_{pixel} are the vertical and horizontal number of pixels respectively. To calculate the error in the rotational angle per pixel from Figure 23[21]:

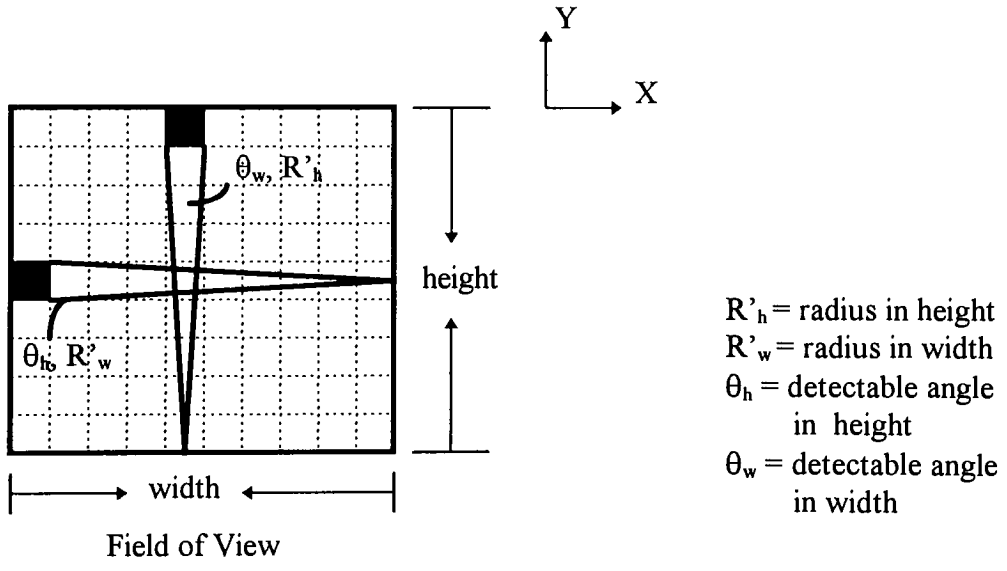

Figure 23: Rotational angle under the pixel array of the camera

$$R_w = R_h^{'}\theta_w \Rightarrow \theta_w = \frac{R_w}{R_h^{'}} = \frac{0.246mm/pixel}{122.7mm} = 2.00 \times 10^{-3} rad = 0.11^\circ \cong 0.1^\circ \quad (8)$$

$$R_h = R_w^{'}\theta_h \Rightarrow \theta_h = \frac{R_h}{R_w^{'}} = \frac{0.253mm/pixel}{123.2mm} = 2.05 \times 10^{-3} rad = 0.12^\circ \cong 0.1^\circ \quad (9)$$

By comparing the threshold value, the vision system can obtain ± 1 pixel accuracy. Therefore, the accuracy of the vision system is approximately ± 0.2 *mm* in the x-direction, ± 0.3 *mm* in the y-direction and ± 0.1° in rotation.

5.3 Vision Recognition

Taking the advantage of the high contrast feature of the PLCC components, binary scale images are used by the vision process to identify their positions and orientations. The vision operation of the robot controller employs the method of prototype model matching to locate the parts. Figure 24 shows the prototype model that is trained to match the actual binary scale image of a PLCC chip. The square boundary including the chamfered corner and the two fiscal marks will determine the PLCC chip's orientation and the area centroid of the image will determine its position under the FOV of the camera. The effort level of the vision recognition is set to 90. That means a 68-pin PLCC chip is considered "found" if the image matches 90% or greater of the prototype model. The vision recognition operation was performed over 40 times and the result shows an average of 97% match in most cases.

digitized binary image

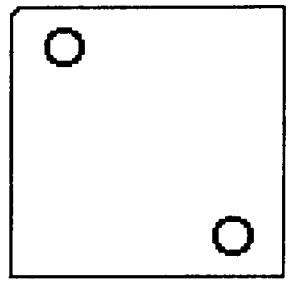

trained prototype model

Figure 24: Prototype training using binary scale image

At the upstream location of the conveyor, a camera is mounted to find the PLCC chips when they come into the FOV of the camera on the moving conveyor. Since the vision system is equipped with the capability of recognizing the positions and orientations of incoming parts, it is essential to provide a good and consistent lighting environment at the picture-taking location. The fluorescent tube used is not industrial grade and has the disadvantage of "flickering." The flicker will result in unstable lighting intensity and will cause an inconsistency in the image acquired, especially in high camera shutter speed. A sheet of gray scale spectrum was used to test the distribution of lighting intensity under the FOV of the camera. Only a rectangular area of about 30% of the FOV area was observed to be an effective area where even lighting intensity can be achieved. Figure 25 shows a pictorial view of the effective area. This observation was done by naked eyes. A much more precise result can be obtained through the use of optical equipment. Since the carrying tray for the PLCC chips are about the same size of the FOV and the FOV covers the entire tray when the picture is taken, it is inevitable that the observed effective region under the FOV is also the only area on the tray that the PLCC chips can be placed to

guarantee consistent image acquisition by the camera. Thus, the capacity of the tray was reduced from the original design of 4 PLCC chips to 2.

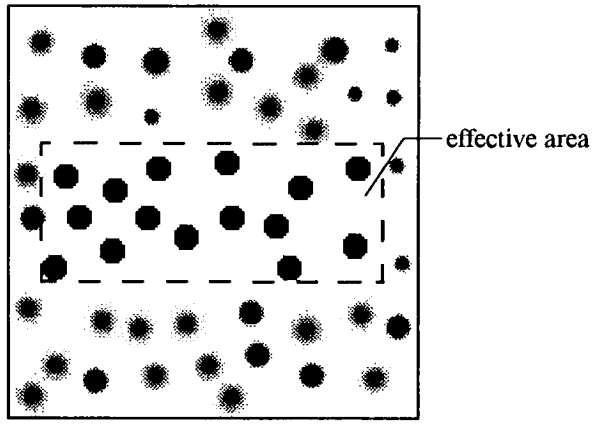

Field of View of the camera (123.2 x 122.7 *mm*)

Figure 25: Distribution of lighting intensity

Another possible solution in achieving consistent lighting distribution is to use a back-lit table rather than the direct lighting method, because the back-lighting can produce the silhouette image of the object that is placed on the table. Unfortunately, back-lighting can not reflect the object's surface characteristics that are critical in recognizing the orientation of the PLCC chip in this case. Also, a back-lit conveyor does not seem to be a common equipment in the industrial workplace.

Because the camera will have to take a picture while the parts are moving, it poses additional difficulty in obtaining clear images of the parts. The conveyor was initially setup to run at about 410 *mm/sec.*[1] At this speed, the camera was unable to get a clear still image of the parts. Although the equipped camera has the capability of higher shutter

[1] Due to the design of the conveyor's mechanism, the conveyor does not move at constant speed.

speed by using the "shuttered, one-field acquisition" option, it will reduce the image resolution by half (only 242 lines high). The reduction in image resolution isn't a feasible option since the pins and chamfered corner of the PLCC chip are very small in size and they are critical features for vision recognition. Therefore, an attempt to reduce the speed of the conveyor was made in an effort to enhance the clarity of the acquiring image. A new DC gearmotor with speed control replaced the AC motor of the conveyor. The speed control is capable of adjusting to 5% to 100% of the maximum rated motor speed. The conveyor was then experimented with at various speeds and finally set to run at about 130 *mm/sec* because this was the maximum speed that the camera was able to acquire clear still images of the parts without losing their resolutions. The speed of the conveyor, in this case, will only affect the vision operation because the encoder tracks the belt distance traveled instead of its running speed.

5.4 Robot Accuracy and End Effector Precision

The robot was tested for its precision and reliability using a pointing rod attached to the end of the quill and a linear displacement gauge. Figure A- 1 in Appendix A-1 shows the published specifications of the AdeptOne SCARA robot. Even though the specifications indicate the possible error from robot's repeatability and the accuracy in the X/Y plane to be ± 0.025 *mm* and in the rotational Joint 4 to be ± 0.05°, the actual test indicated that its maximum error during the test was ± 0.2 *mm* and ± 0.1° respectively.

The test also showed that the run-out of the quill was ± 0.05 *mm*. These sources of errors are very likely to be the result of extensive use of the robot over time.

The design of the end effector assumes that its vertical central axis will align perfectly with the center of the quill (the vertical z-axis). As a matter of fact, the uncertainty resulting from the machining process of the end effector does cause a certain degree of misalignment. Because the end effector was the first prototype and it was not being fabricated under tight tolerance-control conditions, the misalignment resulted in unacceptable inaccuracy as required by the PLCC chip assembly. The misalignment of the end effector is measured to be +1.29 *mm* in the x-direction and +1.26 *mm* in the y-direction. This misalignment can be compensated for by incorporating it into the software program as an end tool offset (see Appendix C-3). After taking the offset into account, the end effector is able to achieve an accuracy of ± 0.1 *mm* in the x-direction and ± 0.2 *mm* in the y-direction. Of course, such misalignment can be minimized by a higher precision machining process during the fabrication of the end effector. Another source of error from the end effector is the rotational angle of its insertion head. Looking at the mechanism of the end effector (see Appendix B-1), even though the circular sliding rod is in a way constrained by the spring force and the rubber o-ring between the slide guide, it does not totally prevent the possible rotation of the insertion head during the extension and retraction of the cylinder pistons. The estimated maximum rotation by direct measurement is about ± 2°. The rotational error can be minimized if a locking mechanism is implemented on the design of the end effector.

The displacement error which may result from the z-axis of the robot is not a primary concern as a source of error in this case since the compressible nature of the air and suction tool's spring-loaded mechanism provide a vertical compliance of over 3 *mm* when the piston rods of the cylinder are extended.

5.5 Overall System Performance

Two PLCC chips of the same type are tracked, recognized, acquired, and inserted into respective PLCC sockets in a single assembly sequence. The same sequence was repeated 30 times. Out of the 30 trials, one PLCC chip was not recognized correctly for its orientation and was forced into the socket and one PLCC chip was not inserted into the socket. The assembly success rate of approximately 93.3% was achieved. The two unsuccessful assembly operations were both the result of incorrect vision recognition. The assembly success rate can definitely be increased by improving the vision operation.

Since the most important idea of conveyor tracking is to increase the production efficiency by eliminating conveyor idling time, the assembly cycle time is a key reference in the determination of the tracking conveyor's efficiency. To make the comparison, the system was also setup to use conveyor indexing to perform the same PLCC chip assembly. Conveyor indexing means the conveyor has to stop for parts acquiring and insertion during assembly operation. Table 5 shows the results of both the conveyor tracking and conveyor indexing systems.

Table 5: Assembly cycle time for tracking and indexing conveyor system

Robot speed = 10%	Conveyor Tracking (*sec.*)	Conveyor Indexing (*sec.*)
Chip Acquisition	1.2	1.1
Vision Operation	1.3	0.8
Chip Insertion	1.7	1.7
Robot Settling Time	0.2	0.1
Tool Dwell Time	0.2	0.1
Conveyor Running Time	9.7	12.3
Total Assembly Cycle Time	**14.3**	**16.1**

For the same assembly operation, a tracking conveyor system shortens the total assembly cycle time by 1.8 seconds as opposed to an indexing conveyor system. That is a 11% improvement in assembly time. Such improvement will be significant when the assembly operation is performed in a large-quantity scale.

The PLCC chips and sockets are measured for their fitting clearance. The shape of both chips and sockets are perfect squares and the clearance is $\pm$ 0.9 *mm* which translates to $\pm$ 4.1° in rotation. These values are treated as the desired accuracy (see Scenario 1 in Figure 26) because the robotic conveyor tracking system has to achieve at least such degree of accuracy for the successful chip assembly operation. Adding up all the possible errors discussed in previous sections, the assembly accuracy can be summarized in Table 6. As a matter of fact, the determination of the system accuracy is a very complicated process which requires the comprehensive analysis of both the hardware design and the software algorithms involved. The accuracy factors shown in Table 6 are estimated values based on the previous discussion rather than the actual representation of the entire system performance.

Table 6: PLCC chips assembly accuracy

Accuracy Factor	translation		rotation
	X (*mm*)	Y (*mm*)	θ (°)
Robot	± 0.2 x 2*	± 0.2 x 2*	± 0.1 x 2*
Vision Recognition	± 0.2**	± 0.3**	± 0.1**
Visual Tracking (Camera-to-Robot)	± 0.1***	± 0.1***	N/A
Conveyor (Robot-to-Conveyor)	± 0.1 x 2*	± 0.01x 2****	± 0.01 x 2****
End Effector	± 0.1*	± 0.2*	± 2*
Overall Accuracy	**± 1.0**	**± 1.0**	**± 2.3**
Desired Accuracy	**± 0.9**	**± 0.9**	**± 4.1**

The errors associated with the robot and the conveyor are counted twice because both parts acquiring and assembly processes are performed using the conveyor tracking technique with the same robot arm. The overall accuracy is the actual performance of the robotic conveyor tracking system. The values shown in this table are all reduced to one significant digit to represent more realistic figures when considering the units associated. Although the overall assembly accuracy does not meet the desired accuracy, successful assembly was still achieved. This was observed to be possible because of the physical structure of the PLCC chips and the sockets. Figure 26 shows the schematic of the scenarios that describe such situation. As mentioned earlier, the PLCC chips have their pins bent around their perimeters so that when inserting the chips, the bent pins provide an extra assembly tolerance in addition to the fitting clearance (see Scenario 2 in Figure 26). That means, the bent pins will slide into and orient the chip itself to the sockets when they

* Values determined by direct measurement.
** Calculated values. See Section 5.2.
*** Calculated values. See Table 4.
**** Values less than 0.01, therefore neglected.

hit the edge of the socket during vertical insertion. Such a "slide-in" situation can only occur when the translation error is no larger than half of the pins' bending radius. By measuring the bending radius of the pin, there is an additional $\pm$ 0.5 *mm* tolerance for the chip insertion process. Thus, as a result, the accuracy that the entire assembly system can achieve is sufficient for the assembly task here.

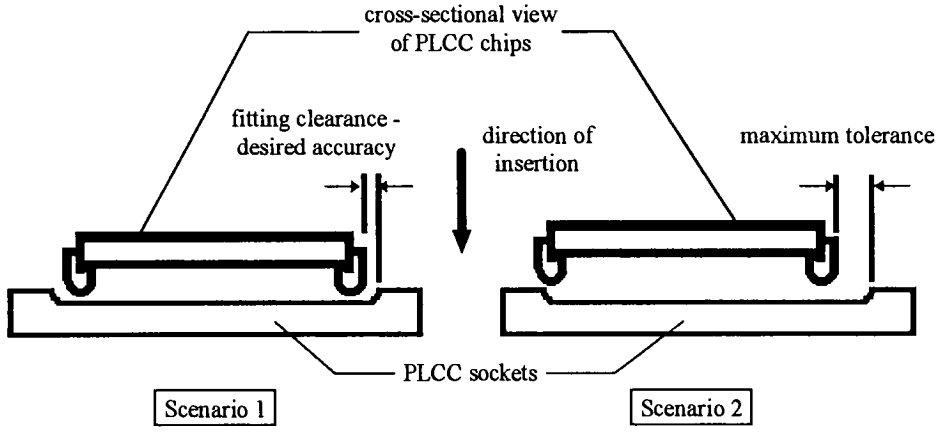

Figure 26: Scenarios of successful chip insertion

6. Future Implementation

To make the whole assembly operation more reliable, several useful features can be implemented to improve the process. For example, an additional camera can be mounted to the downstream location of the conveyor. The workcell then will have the capability of inspecting the assembly result before the parts move out of the assembly line. An additional vision inspection operation can also ensure that the pins on the PLCC chip are not bent incorrectly or damaged before they are assembled.

The AdeptOne robot system has the capability of Optical Character Recognition, or OCR. Unfortunately, the one used here is not equipped with such software feature. With the help of OCR software, the vision system will be able to recognize the identification tag printed on the surface of PLCC chip and instruct the robot to insert it into corresponding PLCC sockets. These printed tags can only be used for chip identification purposes rather than for orientation recognition because they are not always being printed at a exact location of the chip surface.

The conveyor that transports the PLCC chips and circuit board can move at a faster speed if the camera used for the vision operation can accommodate a higher shutter speed. Faster moving speed means the increase in assembly efficiency.

It is certainly beneficial to the assembly accuracy if the end effector is equipped with some type of force sensing capability. The force sensing feature will allow the PLCC chip to be inserted by a more precise force and reduce the chance of damaging the chips and sockets.

7. Conclusions

This paper presents PLCC chip assembly using the non-vision and vision conveyor tracking. The use of the robot with vision system provides a high degree of automation in PLCC chip assembly. Nevertheless, the efficiency and the success rate of the assembly process relies primarily on the accuracy that both the hardware and software of the whole system can achieve. Even though the Adept robot system was already equipped with highly sophisticated software for vision recognition and conveyor tracking operations, the implementation of the hardware components to assist successful assembly operations appeared to be the greatest challenge. The hardware components ranging from the robot's end effector to the motor of the conveyor all played critical roles in the entire assembly process. Overall, the AdeptOne robot with vision guidance system proved itself capable of tracking and assembling small components with the accuracy of $\pm$ 1.0 *mm* in both the x- and y-direction, and $\pm$ 2.3° in rotation. The concept of conveyor tracking is of great industrial applicability and has positive effects on shortening manufacturing time and increasing manufacturing efficiency.

8. References

[1] Tsai, M. C. and Lee, C. H., "Tracking Control of a Conveyor Belt: Design and Experiments," *IEEE Transactions on Robotics and Automation*, vol. 12, no. 1, pp. 126-130, February, 1996.

[2] Papanikolopoulos, N. P., Khosla, P. K., and Kanade, T., "Visual Tracking of a Moving Target by a Camera Mounted on a Robot: A Combination of Control and Vision," *IEEE Transactions on Robotics and Automation*, vol. 9, no. 1, pp. 14-35, February, 1993.

[3] Tomkins, J. A. and White J. A., Facilities Planning, Wiley, New York, 1984.

[4] Asimov, I. and Frenkel, K. A., Robots - Machines in Man's Image, Harmony Books, New York, 1985.

[5] Adept Technology, Inc., Adept MotionWare User's Guide, Adept, San Jose, February, 1992.

[6] Adept Technology, Inc., Adept VisionWare User's Guide, Adept, San Jose, February, 1992.

[7] Holst, G. C., CCD Arrays, Cameras, and Displays, JCD Publishing, Winter Park, Florida, 1996.

[8] Rosch, W.L., The Hardware Bible , 3rd ed., Sams Publishing, Indianapolis, 1994.

[9] Zhang, W. and Ralescu, A., "Object Recognition Based on Pattern Features," *Advances in Intelligent Computing - IPMU '94. 5th International Conference on Information Processing and Management of Uncertainty in Knowledge-Based Systems*, pp. 567-576, 1995.

[10] Denker, A., Sabanovic, A., and Kaynak, O., "Vision-Controlled Robotics Tracking and Acquisition," *IROS '94. Proceedings of the IEEE/RSJ/GI International Conference on Intelligent Robot and Systems*, vol. 3, pp. 2000-2006, 1994.

[11] Allen, P. K., Timcenko, A., Yoshimi, B., and Michelman, P., "Automated Tracking and Grasping of a Moving Object with a Robotic Hand-eye System," *IEEE Transactions on Robotics and Automation*, vol. 9, no. 2, pp. 152-165, April, 1993.

[12] Doignon, C., Abba, G., and Ostertag, E., "Recognition and localization of solid objects by a monocular vision system for robotic tasks," *IROS '94. Proceedings of the IEEE/RSJ/GI International Conference on Intelligent Robots and Systems*, vol. 3, pp. 2007-2014, 1994.

[13] Chin, R. T. and Dyer, C. R., "Model-Based Recognition in Robot Vision," *ACM Computing Surveys*, vol. 18, no. 1, pp. 67-103, March, 1996.

[14] Baird, M. L., "Sight I: A Computer Vision System for Automated IC Chip Manufacture," *IEEE Transactions on Systems, Man, and Cybernetics*, vol. 8, no. 2, pp. 133-139, February, 1978.

[15] Agin, G. J., "Computer Vision Systems for Industrial Inspection and Assembly," *Computer*, vol. 13, no. 5, pp. 11-20, May, 1980.

[16] Lyman, J., "Low-Cost Plastic Frame Reliably Mates Leadless Chip-Carrier and Printed Circuit Board," *Electronics*, vol. 56, no. 25, pp. 48-50, December, 1983.

[17] Tam, S. C., Noor, Y. M., Lim, L. E. N., Jana, S., Yang, L. J., Lau, M. W. S., and Yeo, C. Y., "Marking of Leadless Chip Carriers with a Pulsed Nd: YAG Laser," *Proceedings of the Institute of Mechanical Engineers*, part B., vol. 3, pp. 179-192, 1993.

[18] Makino, H. and Furuya, N., "The SCARA Robot and Its Family," Robotic Assembly, Rathmill, K. ed., pp. 13-26, IFS Publications, 1985.

[19] Tech Tran Corporation, Industrial Robots - a Summary and Forecast, pp. 124-125, Tech Tran Corporation, Naperville, IL, 1983.

[20] Aleksander, I., Stonham, T. J., and Wilkie, B. A., Computer Vision Systems for Industry: Comparisons. In Artificial Vision for Robots, pp. 179-196, Chapman and Hall, New York, 1984.

[21] Hsu, Y. H., "Adept Robot Vision System and Magnet-Type End Effector Used for Integrated Circuit Component Assembly," Master Thesis, Department of Mechanical Engineering, Rochester Institute of Technology, 1996.

[22] Miller, R. K., Machine Vision for Robotics and Automated Inspection, vol. III, 3rd ed., SEAI Technical Publications, 1985.

[23] Luo, R. C., Mullen, R. E., Jr., and Wessel, D. E., "An Adaptive Robot Tracking System Using Optical Flow," *Proceedings of IEEE International Conference on Robotics and Automation*, pp. 568-573, 1988.

[24] Park, T. H. and Lee, B. H., "An Approach to Robot Motion Analysis and Planning for Conveyor Tracking," *IEEE Transactions on Systems, Man, and Cybernetics*, vol. 22, no. 2, March/April, 1992.

[25] Holland, S. W., Rossal, L., and Ward, M. R., "CONSIGHT-1: A Vision Controlled Robot System for Transferring Parts from Belt Conveyors,", *Computer Vision and Sensor-Based Robots*, Dodd, G. G. and Rossal, L., eds, Plenum, New York, 1979.

[26] Allen, P. K., "Real-Time Motion Tracking Using Spatio-Temporal Filters," *Proceedings of DARPA Image Understanding Workshop*, pp. 695-701, 1989.

[27] Paul, R. P., "Manipulator Cartesian Path Control," *IEEE Transactions on Systems, Man, and Cybernetics*, vol. SMC-9, pp. 702-711, 1979.

Appendix A. Technical Data

A-1 AdeptOne SCARA Robot

A-2 Adept CC Controller

A-3 Infrared Sensors

A-4 CCD Camera

A-5 Gearmotor and Speed Control Used to Drive the Conveyor

A-6 Conveyor

A-7 Belt Encoder

A-8 Digital I/Os

A-1 AdeptOne SCARA Robot

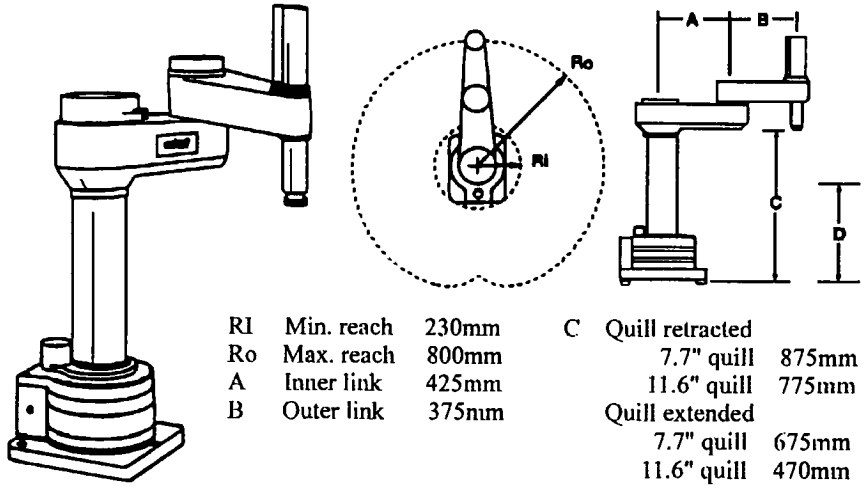

RI	Min. reach	230mm	C	Quill retracted	
Ro	Max. reach	800mm		7.7" quill	875mm
A	Inner link	425mm		11.6" quill	775mm
B	Outer link	375mm		Quill extended	
				7.7" quill	675mm
				11.6" quill	470mm

Figure A- 1: AdeptOne robot and its work envelope [5]

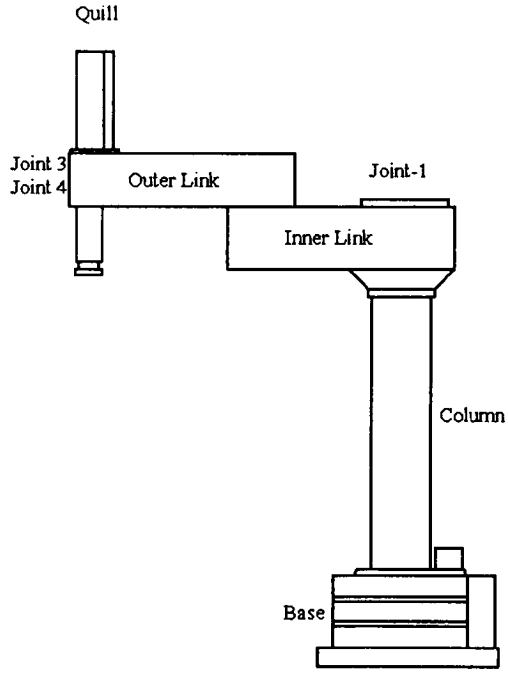

Figure A- 2: SCARA robot terminology

Table A- 1: AdeptOne robot performance specifications[1]

Reach	
Maximum radial	31.5 *in.*(800 *mm*)
Minimum radial	9.0 *in.* (229 *mm*)
Vertical clearance (base bottom to end effector flange) Standard 7.7 *in.* stroke	
- with maximum Joint 3 retraction	34.52 *in.* (877 *mm*)
- with maximum Joint 3 extension	26.75 *in.* (679 *mm*)
Vertical Stroke - Z direction (standard Joint 3)	7.7 *in.* (196 *mm*)
Joint Rotation	
Joint 1	300°
Joint 2	294°
Joint 3	554°
Payload during operation (including end effector)	20 *lb.* (9.1 kg)
Inertia Load About Joint 4 axis - standard (Maximum)	96 *lb-in*^{2} (0.28 *N-m*^{2})
Force (Joint 3 downward force without payload)	40 *lb.* (18.2 *kg*)
Torque (Joint 4)	60 *lb-in* (6.78 *N-m*)
Cycle Time-12 *in.* (305 mm) 1 *lb.* (0.45 *kg*) / 20 *lb.* (9.1 *kg*)	0.9 *sec* / 1.7 *sec*
Resolution	
Joint 1	0.00078°
Joint 2	0.00312°
Joint 3	0.00013 *in.* (0.0033 *mm*)
Joint 4	0.047°
Repeatability	
X, Y plane	±0.001 *in.* (±0.025 *mm*)
Joint 3 (vertical Z)	±0.002 *in.* (±0.050 *mm*)
Joint 4 (rotational)	±0.05°
Accuracy in X/Y Plane (at ±3° F with HPS over 17"x17")	±0.003 *in.* (±0.076 *mm*)
Joint Speed (maximum)	
Joint 1	540°/sec
Joint 2	540°/sec
Joint 3	19.7 *in/sec* (500 *mm/sec*)
Joint 4	3600°/sec
Robot Weight (without options)	400 *lb.* (182 *kg*)
Design Life	42,000 hours

[1] Source: AdeptOne technical specifications

A-2 Adept CC Controller

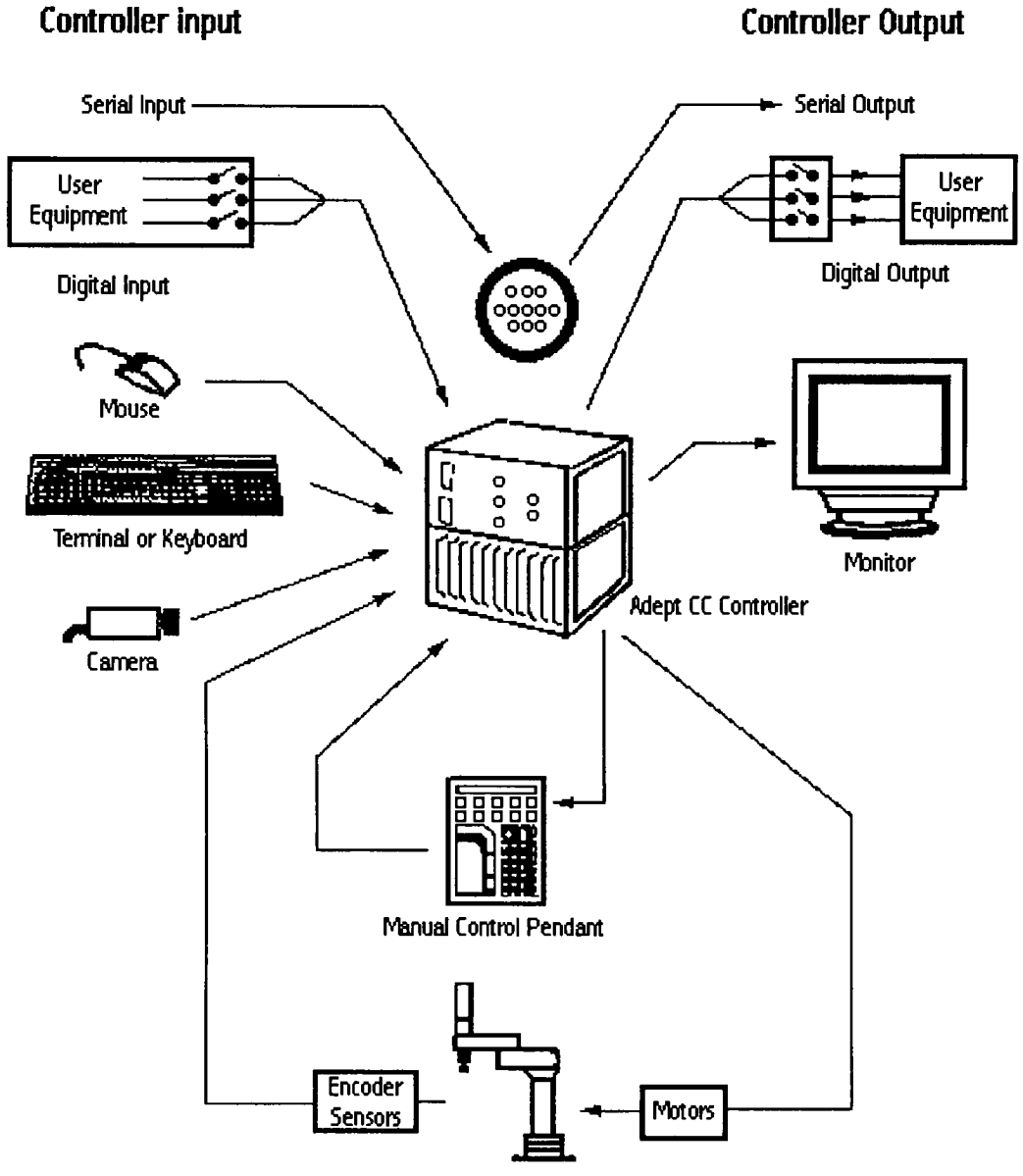

Figure A- 3: Adept CC controller and peripherals[1]

[1] Source: Adept VisionWare User's Guide

A-3 Infrared Sensors

Manufacture: Data Logic DL optic electronics

Model: ET3-03

S/N: 646061 (upstream)

S/N: 542676 (downstream)

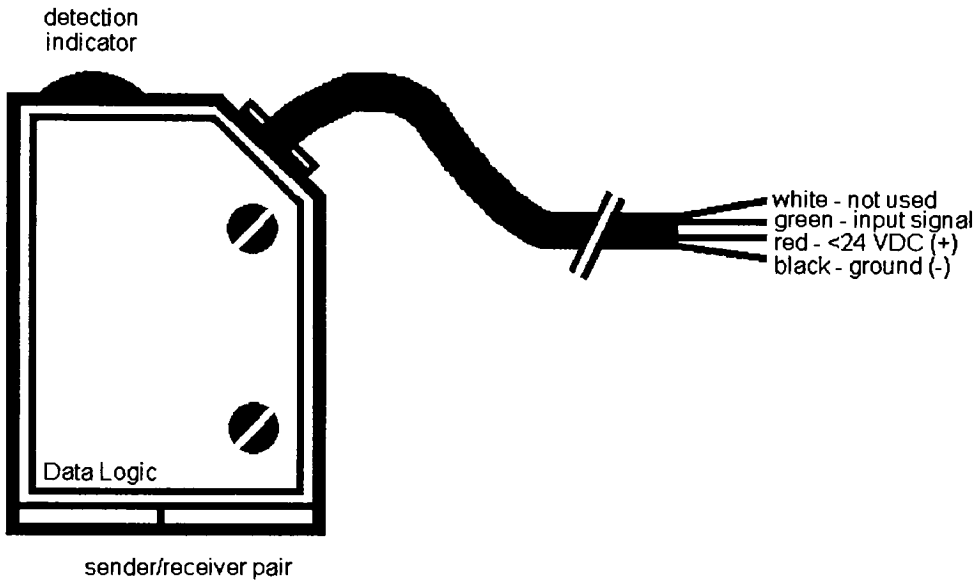

Figure A- 4: Diagram of the infrared optical sensor

A-4 CCD Camera

Table A- 2: General specification of the CCD camera

Manufacture	Panasonic
Model	GP-CD40
Type	charged coupled device
Resolution	501 x 485 pixels
Image	gray scale or binary
Image Acquired Time	1/30 or 1/60 *sec.*
Shuttered Mode	1/1000 *sec.* fixed
Lens	25 *mm*
Mounting	stationary
Mounting Height (camera lens to conveyor surface)	630.3 *mm*
Connection	Adept CC controller physical camera port 1

With shuttered cameras, the strobe signal is used to latch the external encoders of motion devices simultaneously with image acquisition. Since the timing for a strobe signal used to record encoder positions is different from the timing for a strobe light, cameras used in shuttered cameras cannot be used with strobe lights.

A-5 Gearmotor and Speed Control Used to Drive the Conveyor

Table A- 3: Dayton gearmotor specifications[1]

Dayton Gearmotor	
Model	4Z538A
Motor Type	permanent magnet DC motor
Input HP	1/30
Voltage	90 *VDC*
RPM F/L	50
Torque F/L	26 *in-lb.*
Gear Ratio	63 : 1
Mounting Type	face
Shaft Size	5/16" diameter
Motor	TENV
Duty	continuous
Ambient Temperature	40°*C* maximum
Insulation	class A
Bearing	sleeve - motor sleeve - gearbox

Table A- 4: Dayton DC motor control specifications[2]

Dayton DC Motor Control	
Model	6A191
Max. Ambient Temperature for Control	40°*C*
Control Input	115 *VAC* + 10% - 5%, 60 *Hz*, single phase, 3 *A* (max.)
Control Armature Supply Output	0 to 90 *VDC*, 3 *A* (max.)
Rated for use with ONLY DC Permanent Magnet Gearmotor / Motors	1/35 to 1/6 *HP*
Control Motor Speed Regulation	within 30% of motor base speed (speed of motor at rated armature voltage)
Control Motor Speed Range	0 to base speed (15 : 1 constant torque)

[1] Source: Dayton gearmotor operating instructions & parts manual
[2] Source: Dayton DC motor control operating instructions & parts manual

A-6 Conveyor

Table A- 5: Conveyor general specifications

Manufacture	Dorner
Type	4100 series
Belt Length	60 *in.*
Belt Width	6 *in.*
Height	2 *in.*
Movement	bi-directional
Mechanism	shaft driven

A-7 Belt Encoder

Table A- 6: Encoder general specifications[1]

Mechanical	
Dimension	See encoder reference manual
Weight	4 *ounces*
Acceleration	500,000 *rad/sec*^{2} max.
Shaft size	0.2479 +0000/-0002
Shaft load	Axial 10 *lb.* Radial 10 *lb.*
Electrical	
Code	incremental
Cycles per revolution	120 to 1024 on code disc
Supply voltage	+ 5 *Volts* ± 10% @ 60 *ms*
Output format	dual channel, quadrature ± 30° electrical
Output format options	index and dual resolution
Output type	square wave TTL, 20 MA sink 0.4 *V* Max. 10 MA source 3.5 *V* Min.
Frequency response	data 100 *kHz*
Frequency response	index 40 *kHz*
Environmental	
Temperature	operating 0° to 80°*C* storage -25° to 90°*C*
Shock	50 *G's* for 11 *ms* duration
Vibration	5 to 2 *kHz* @ 20 *G's*

[1] Source: Adept technical support

A-8 Digital I/Os

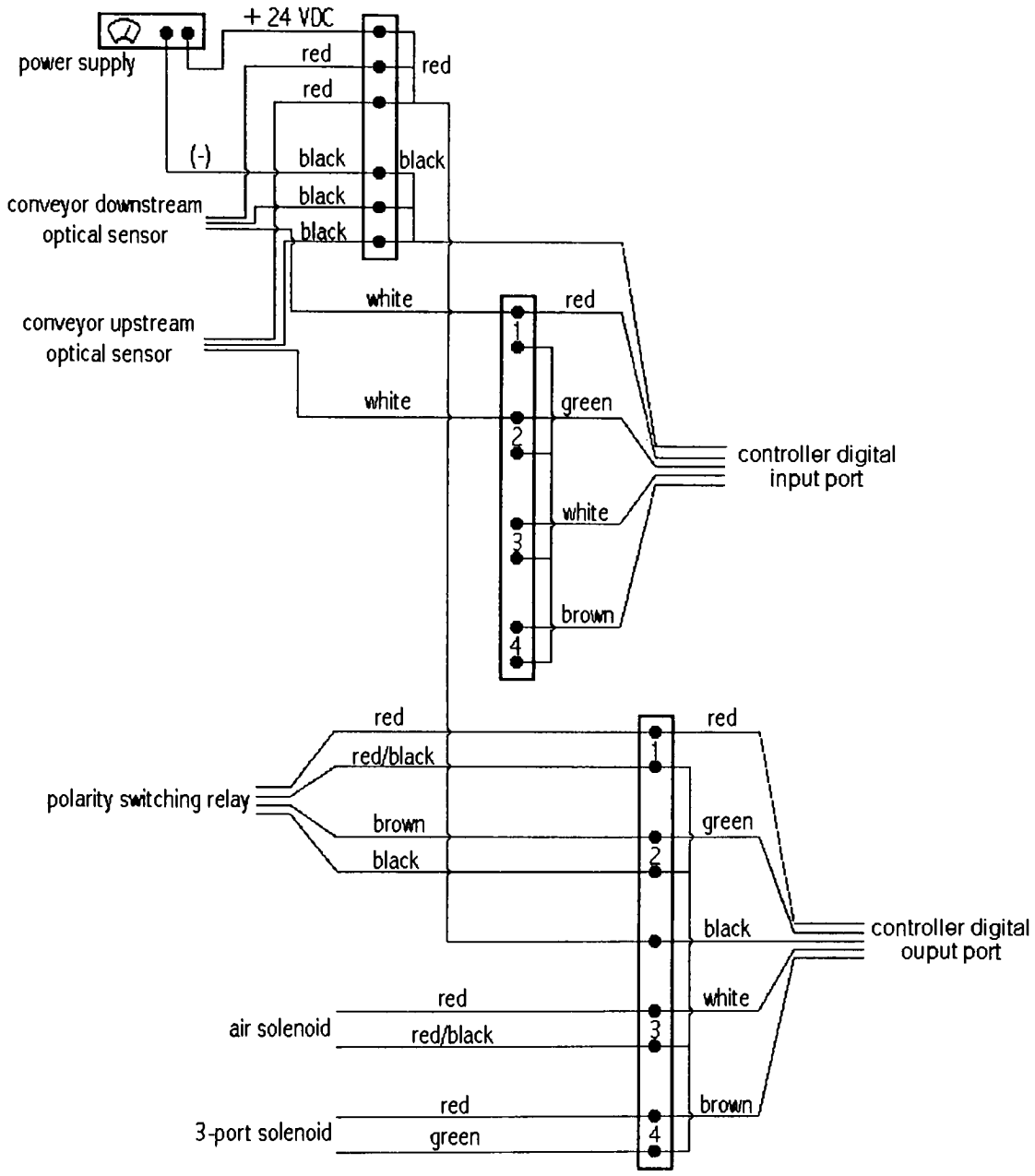

Figure A- 5: Wiring diagram of the digital I/Os

Appendix B. End Effector CAD Drawings

B-1 Assembly Drawing

B-2 Adapter Plate

B-3 Cylinder Support Plate

B-4 Cylinder Mount

B-5 Sliding Rod

B-6 Slide Guide

B-7 Insertion Head Piece

B-8 Insertion Head Cover Piece

B-1 Assembly Drawing

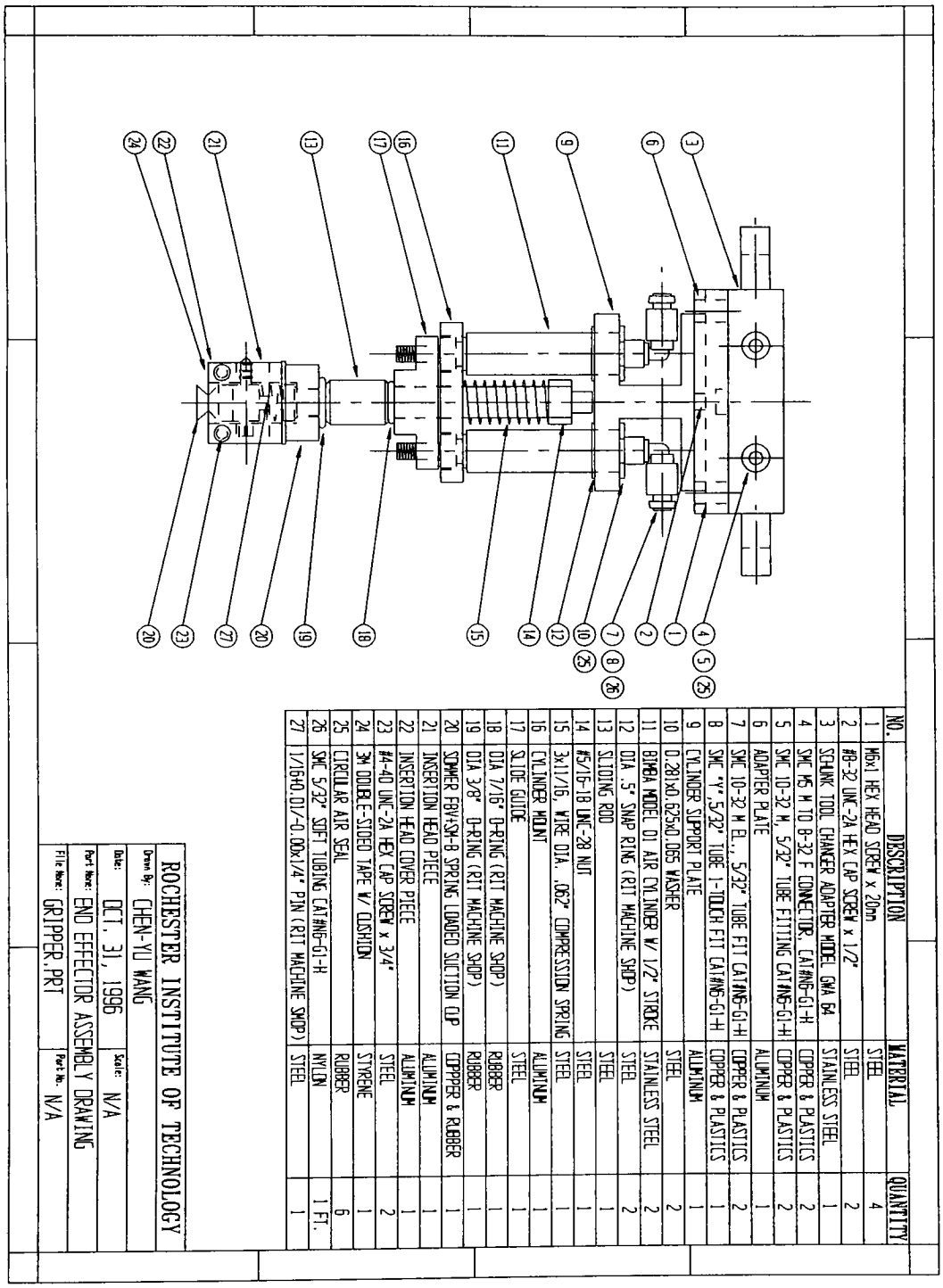

NO.	DESCRIPTION	MATERIAL	QUANTITY
1	M6x1 HEX HEAD SCREW x 20mm	STEEL	4
2	#8-32 UNC-2A HEX CAP SCREW x 1/2"	STEEL	2
3	SCHUNK TOOL CHANGER ADAPTER MODEL GWA 64	STAINLESS STEEL	1
4	SMC M5 M TO 8-32 F CONNECTOR, CAT#NG-G1-H	COPPER & PLASTICS	2
5	SMC 10-32 M, 5/32" TUBE FITTING CAT#NG-G1-H	COPPER & PLASTICS	2
6	ADAPTER PLATE	ALUMINUM	1
7	SMC 10-32 M EL., 5/32" TUBE FIT CAT#NG-G1-H	COPPER & PLASTICS	2
8	SMC "Y", 5/32" TUBE I-TOUCH FIT CAT#NG-G1-H	COPPER & PLASTICS	1
9	CYLINDER SUPPORT PLATE	ALUMINUM	1
10	0.281xO.625xO.065 WASHER	STEEL	2
11	BIMBA MODEL 01 AIR CYLINDER W/ 1/2" STROKE	STAINLESS STEEL	2
12	DIA .5" SNAP RING (RIT MACHINE SHOP)	STEEL	2
13	SLIDING ROD	STEEL	1
14	#5/16-18 UNC-2B NUT	STEEL	1
15	3x11/16, WIRE DIA. .062" COMPRESSION SPRING	STEEL	1
16	CYLINDER MOUNT	ALUMINUM	1
17	SLIDE GUIDE	STEEL	1
18	DIA 7/16" O-RING (RIT MACHINE SHOP)	RUBBER	1
19	DIA 3/8" O-RING (RIT MACHINE SHOP)	RUBBER	1
20	SOMMER FBV45M-B SPRING LOADED SUCTION CUP	COPPER & RUBBER	1
21	INSERTION HEAD PIECE	ALUMINUM	1
22	INSERTION HEAD COVER PIECE	ALUMINUM	1
23	#4-40 UNC-2A HEX CAP SCREW x 3/4"	STEEL	2
24	3M DOUBLE-SIDED TAPE W/ CLOSHION	STYRENE	1
25	CIRCULAR AIR SEAL	RUBBER	6
26	SMC 5/32" SOFT TUBING CAT#NG-G1-H	NYLON	1 FT.
27	1/16HO.01/-0.00x1/4" PIN (RIT MACHINE SHOP)	STEEL	1

ROCHESTER INSTITUTE OF TECHNOLOGY	
Drawn By: CHEN-YU WANG	
Date: OCT. 31, 1996	Scale: N/A
Part Name: END EFFECTOR ASSEMBLY DRAWING	
File Name: GRIPPER.PRT	Part No.: N/A

B-2 Adapter Plate

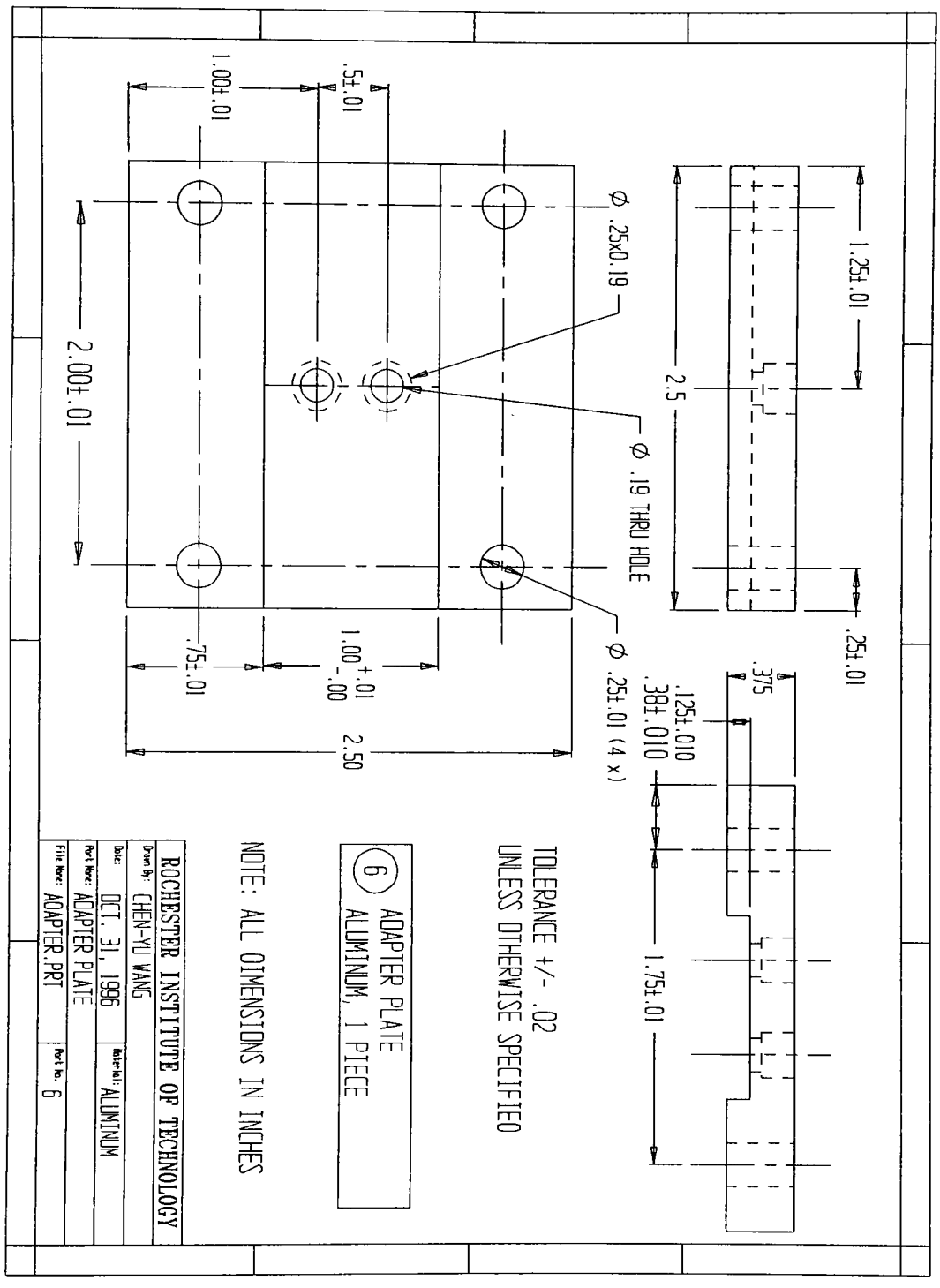

B-3 Cylinder Support Plate

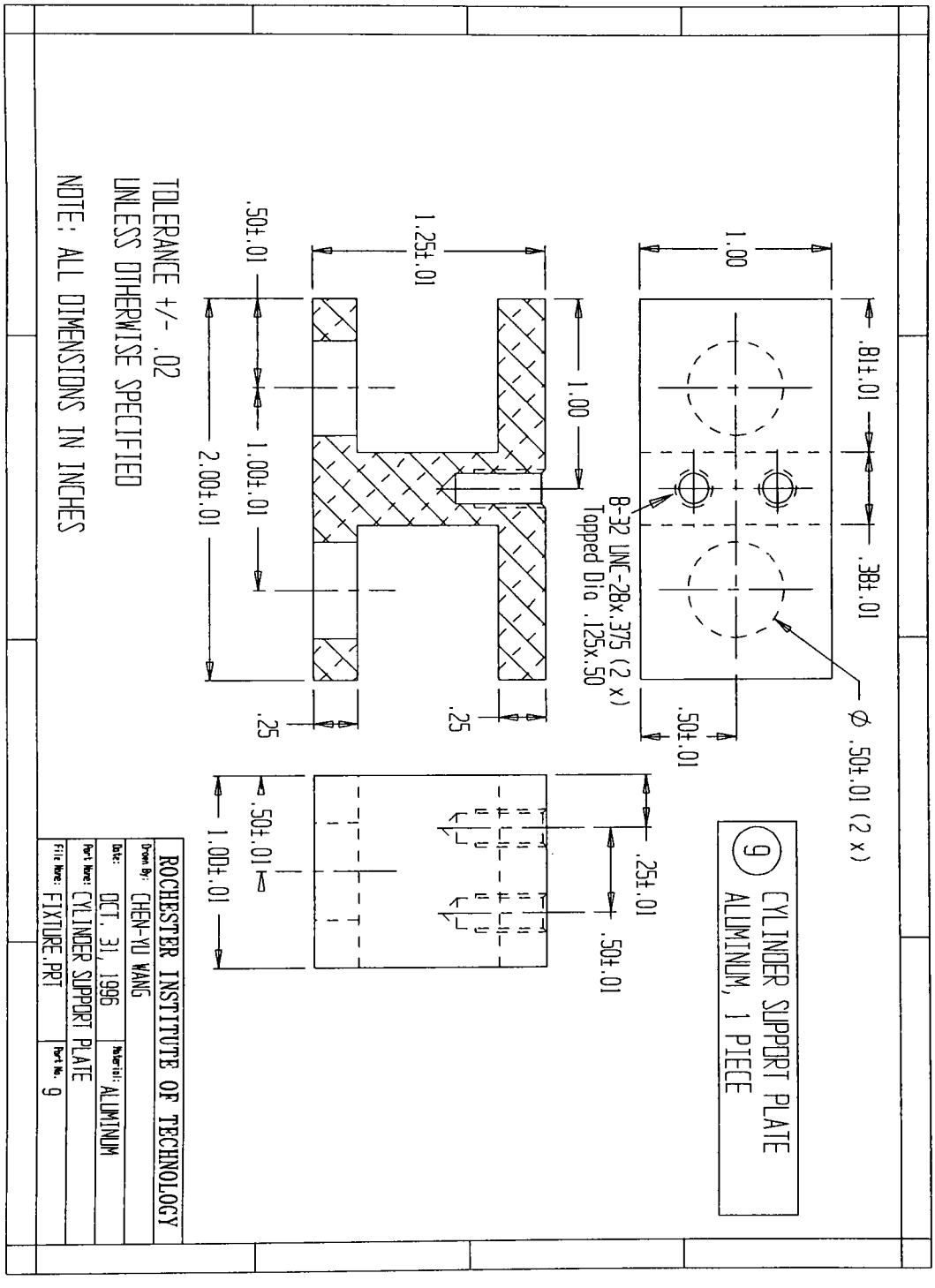

B-4 Cylinder Mount

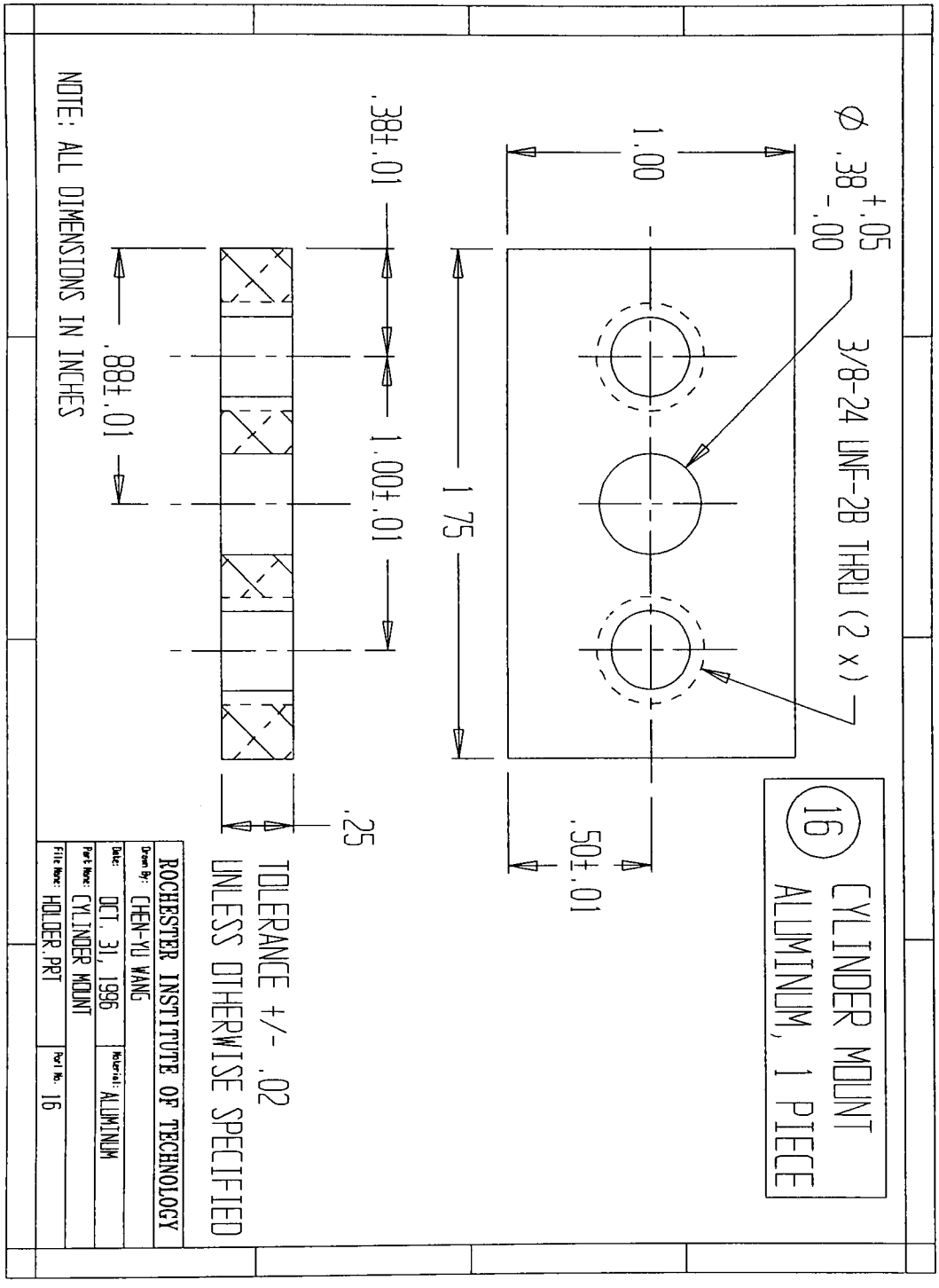

B-5 Sliding Rod

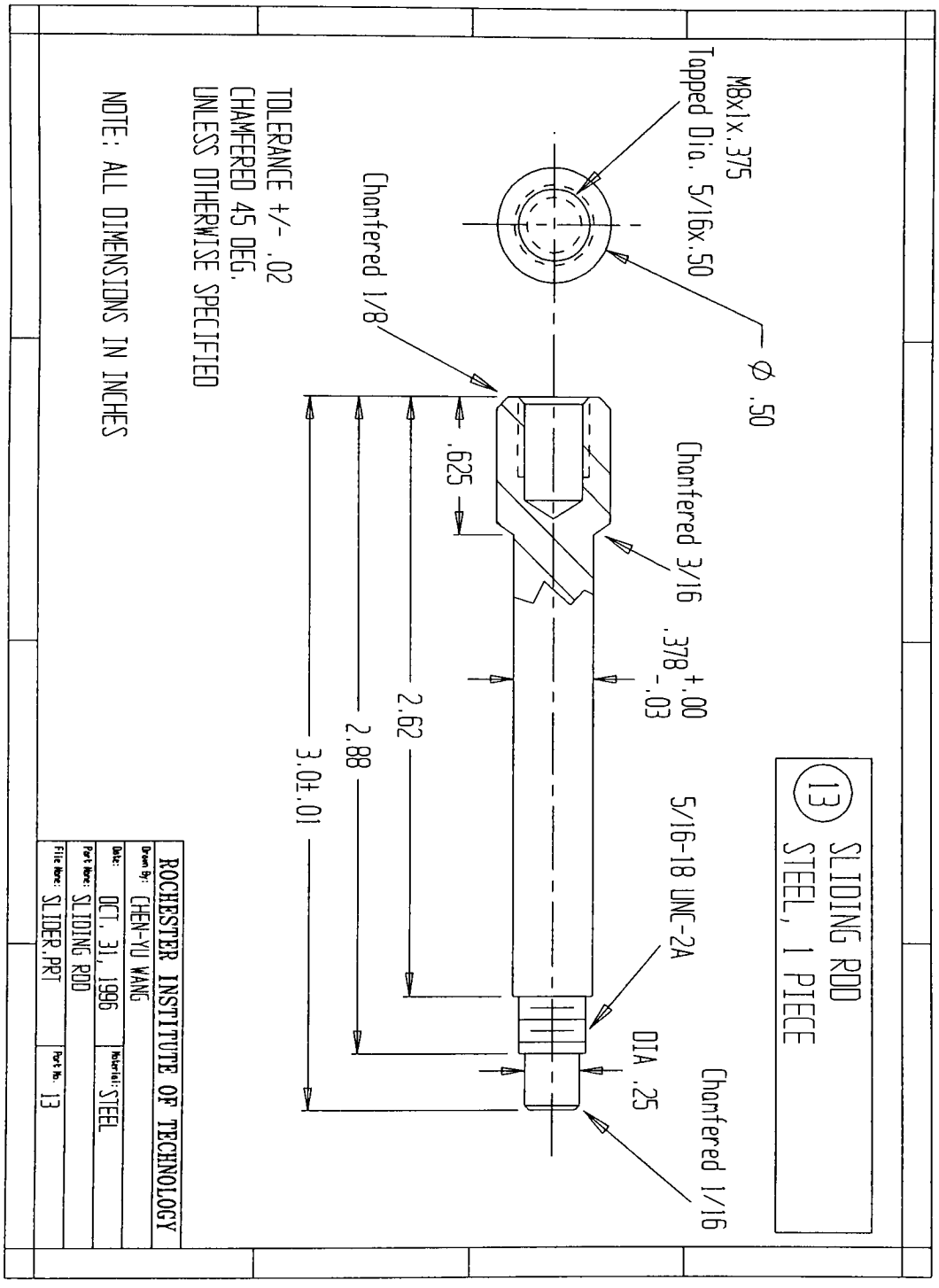

B-6 Slide Guide

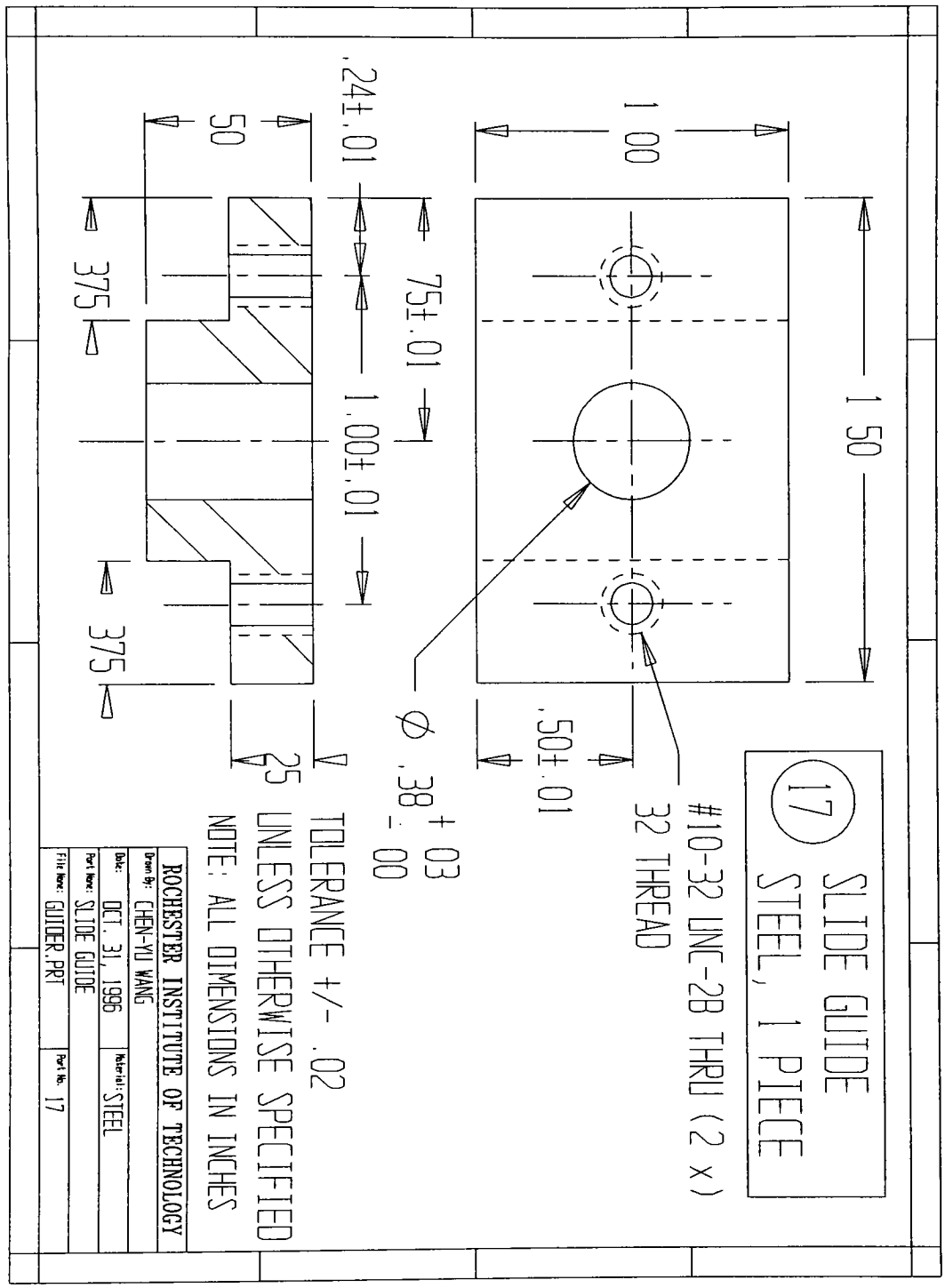

B-7 Insertion Head Piece

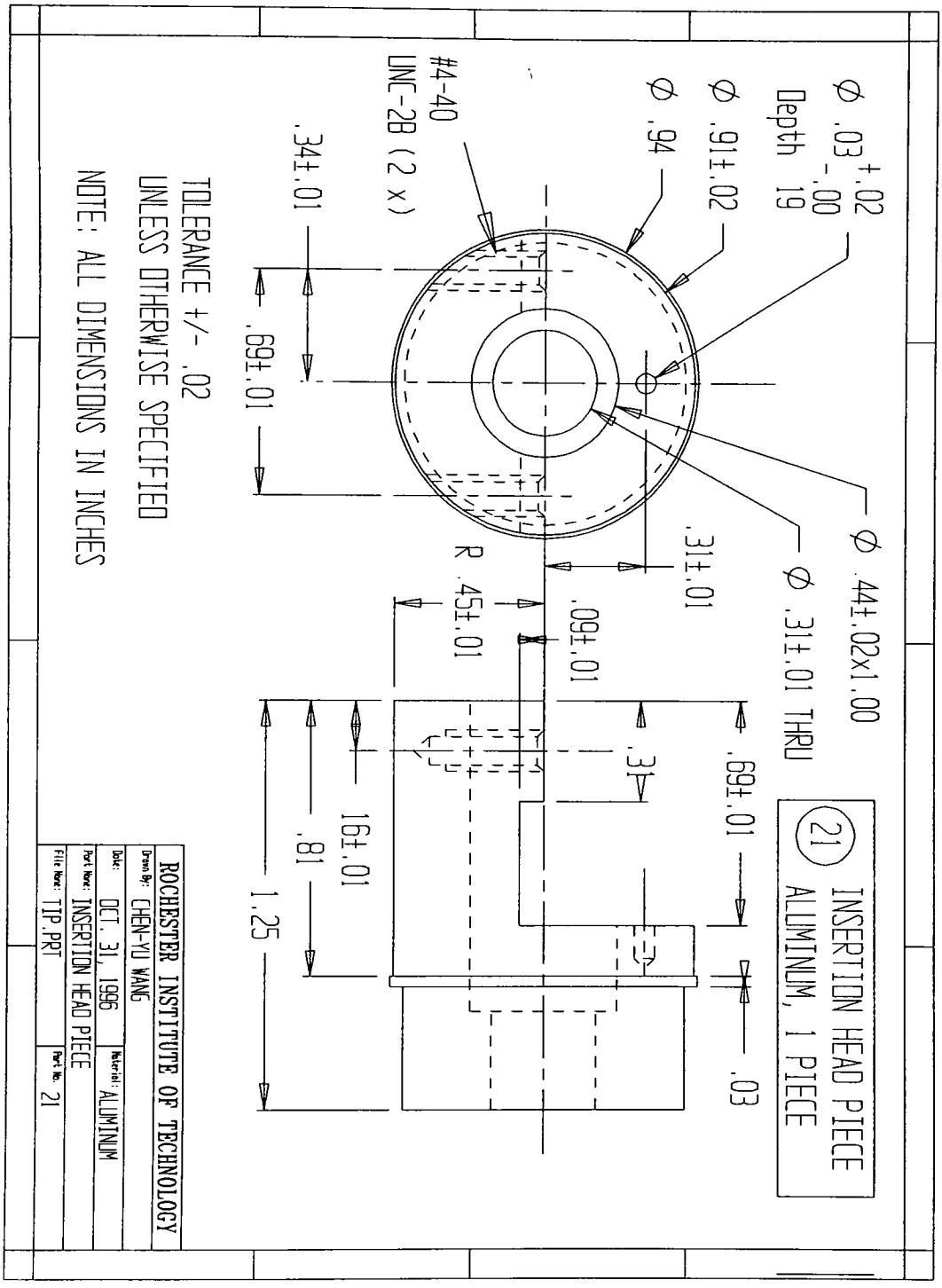

B-8 Insertion Head Cover Piece

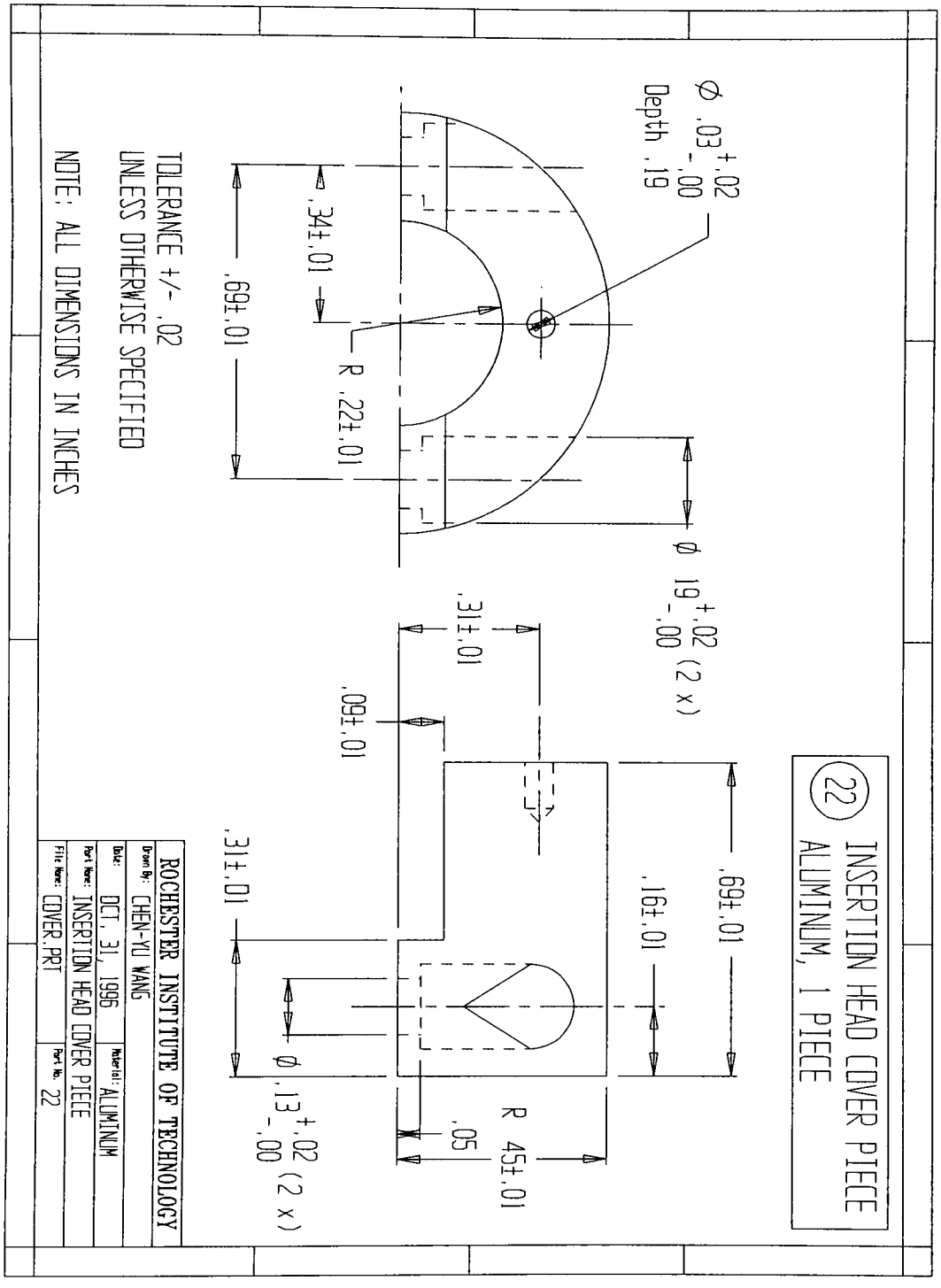

Appendix C. Vision & Non-Vision Conveyor Tracking Programming

C-1 General Information and System Startup

C-2 Conveyor, Camera Calibrations and Reference Frame Creation

C-3 Tool Transformation Creation

C-4 Example Sequence

C-1 General Information and System Startup

Appendix C explains the essential steps in programming the AdeptOne robot to perform non-vision and vision conveyor tracking for the PLCC chip assembly discussed in this thesis. For clarity, all system commands are in **bold** face and should be entered exactly as they appear and followed by a "↵ " carriage return symbol. Menu selectable items are in *italic* font and can be selected using the middle button on the mouse. A "⇒" symbol indicates the sequence of selecting menu items. MCP stands for Manual Control Pendant. It is used to move the robot arm to specific locations. Before using, the MCP should be switched to "manual" mode and returned to "computer" mode when done. Before any programming begins, all the supplementary hardware should be properly setup.

- To start the robot system, make sure the key on the robot controller is switched to "terminal" mode.
- Turn on the monitor and the robot controller. All the Light Emitting Diodes, or LEDs, on the MCP should flash quickly. If not, turn off the robot controller and restart again.
- After several minutes of system initialization, a "." prompt should appear on the monitor screen and the Liquid Crystal Display, or LCD, screen on the MCP should read "NO PROGRAM PRIMED".
- Type **enable power** ↵ (or **en p** ↵) to power up the robot arm.
- Type **calibrate** ↵ (or **ca** ↵) to calibrate the robot.

CAUTION: The robot arm will move.

C-2 Conveyor, Camera Calibrations, and Reference Frame Creation

MotionWare and VisionWare are Adept Assembly Information Management, or AIM, modules with Graphic User Interface, or GUI, which allow menu-driven user-friendly programming of robot motion and vision operation on the AdeptOne robot.

- To start AIM, first type **def d=c:\aim** to change the working directory to where AIM resides.
- Type **load lmow** to load both MotionWare and VisionWare modules into memory.
- Type **comm lmow** to execute the modules.
- Enter the time and date in the requested format when prompted.

Once the execution is complete and system is ready, a windows-like GUI will appear on the screen. The menu functions are arranged on the top of the screen and is called the Main Menu Bar, or MMB. A smaller window will pop up when a menu item is selected. The menu functions in the small window is called the Window Menu Bar, or WMB. Before calibrating the conveyor and the camera, a calibration pointing rod should be attached to the end of robot quill and a calibration disc should be ready for use.

- Select *Edit* $\Rightarrow$ *Frame* on the MMB and then *Edit* $\Rightarrow$ *New* on the WMB to create a new reference frame.
- Type in a name for the new reference frame (ex. vision_track) and click on "Indexing" and "Vision" options. Give a description of the reference frame. This reference frame is for vision tracking conveyor.

- Select *Set-Up⇒ Calibrate Conveyor* on the MMB to calibrate the conveyor.
- From the pick list displayed, select the new reference frame record you just created to calibrate.
- The calibration instruction will be displayed. Follow the instruction step by step to complete the conveyor calibration.
- When finishing, exit the conveyor calibration program and select *Utilities⇒ Load/Store Belt Data* on the MMB and then select the name of the reference frame just calibrated to save it on a disk file. Name the file according to the "BELTxxx.DAT" convention, where xxx is a number from 1 to 999 (ex. BELT777.DAT).
- Select *Edit ⇒ Frame* on the MMB and then *Seek ⇒ Index* on the WMB and use the mouse to double click on the vision tracking conveyor frame just calibrated.
- Define the belt window lower and upper limits.
- To create another reference frame for the non-vision tracking conveyor, select *Edit ⇒ Copy Record ⇒ Paste Record* on the WMB.
- A new reference frame with the same conveyor calibration data is created. Give it a different name (ex. nonvision_track) and deselect the "Vision" option and define the belt window limits.
- Exit AIM by selecting *Special ⇒ System Shutdown* on the MMB.
- Type **def d=c:\util** to change the working directory to where the camera calibration resides.

- Type **load adv_cal** to load the advanced camera calibration program into memory.
- Type **ex a.adv_cal** to execute the camera calibration program.
- Press ↵ to use the default 1 virtual camera to work with.
- Press ↵ to use the default 1 physical camera to use.
- Enter **3** from the menu options to calibrate the current camera.
- Enter **5** from the calibration configuration menu.
- Type **c:\aim** ↵ to indicate the directory where the belt calibration file is stored.
- Enter the "number" of the belt data to use (ex. 777).
- Answer **Y** ↵ to proceed the camera calibration.

Follow the instruction display on the screen and complete the camera calibration. Adjust the video parameter when necessary in order to obtain the best image of the calibration disc. There are several things you should be careful of. Make sure that the camera's type and acquire mode are "Normal Camera" and "Full Frame Acquire", which allow the camera to acquire an image using its highest resolution. When there is a need to advance the conveyor, a monitor command window can be activated to input I/O commands by selecting *Adept* ⇒ *Monitor* on the upper right corner. Under the monitor command window, type **sig "I/O number"** ↵ to turn on/off a digital signal (ex. **sig 9** ↵ to turn on the and **sig -9** ↵ to turn off the conveyor). For best results, the calibration disc should be taped to the belt or carrying tray surface when transported on the conveyor. When the conveyor surface is not perfectly perpendicular to the camera's facing direction, perspective calibration should be used to improve calibration result.

- When finishing, remember to save the camera calibration data to a disc file. The naming convention is "AREAxxx.DAT" where xxx is a number from 1 to 999 (ex. BELT777.DAT).
- Exit the advanced camera calibration program and return to the "." prompt.
- Type **zero** ↵ and **Y** ↵ to remove the calibration program from memory.
- Reload the AIM modules by typing **def d=c:\aim** ↵ , **lo lmow** ↵ , and **comm lmow** ↵.
- Select *Special* ⇒ *Edit Init Data* on the MMB and then select *VISINI.DB* to change the vision initialization.
- Replace the camera data file to the one you just calibrated (ex. AREA777.DAT) and then exit the system by selecting *Special* ⇒ *System Shutdown* on the MMB.
- Reload the AIM modules by typing **def d=c:\aim** ↵ , **lo lmow** ↵ , and **comm lmow** ↵ and now both MotionWare and VisionWare are ready for programming with the new conveyor and camera calibration data you just created.

Note: If the robot, camera, or conveyor is moved in anyway later on, the calibration procedures described in this section should be repeated to ensure the vision and non-vision conveyor tracking operation accuracy.

C-3 Tool Transformation Creation

When the vertical central axis of the end effector is not perfectly aligned to the center of the robot tool flange, or the quill, a tool transformation becomes necessary in order to compensate for the offset. The offset should be measured or calculated from the end effector's dimensional specification before creating the tool transformation.

- To create a tool transformation, select *Edit* ⇒ *Tool* on the MMB and select *Edit* ⇒ *New* on the WMB.
- Enter a name for the tool record and input the values of the end effector's offset with respect to the center of the tool flange in millimeters. Then, choose the tool either as tool 1, 2, or 3 by pressing the corresponding button.
- Click on the corresponding *Set* bottom to set the current tool to the tool transformation just specified.

Whenever the AIM modules are restarted, the *set* bottom needs to be clicked again to set the current tool to the specified offset values unless the optional {USING tool} clause of a sequence statement is specified.

C-4 Example Sequence

```
************************************************************
The following is the sample program sequence used for the
conveyor tracking system discussed in this paper.
************************************************************
Refer to Table 1 for a list of I/O signals. Names staring with
loc_* refer to robot locations which are taught by the
programmer. Names ending with *_track are dynamic conveyor
reference frames relative to the robot location. Words in
bold UPPERCASE are program commands. Refer to Adpet
MotionWare and VisionWare User's Guide for creating the
location, vision , and sequence records.
************************************************************
Initializing I/O signals.
  1. IO OUTPUT -2001
  2. IO OUTPUT -2031
  3. IO OUTPUT -2041
  4. IO OUTPUT -2042
  5. IO OUTPUT -9
  6. IO OUTPUT -10
  7. IO OUTPUT -11
  8. IO OUTPUT -12
Move the robot to a nominal location before starting.
  9. MOVE_TO loc_nominal
Attach vision and non-vision conveyor reference frame to
robot world coordinate.
 10. ATTACH_FRAME vision_track TO VISION fin_chip TAG 2041
 11. ATTACH_FRAME nonvision_track
 12. CHECK_FRAME vision_track AND nonvision_TRACK
 13. IO OUTPUT 11
Staring the conveyor
 14. IO OUTPUT 2001
 15. WAIT_FOR 2001 OUTPUT 9
Wait until PLCC chip carrying tray triggers upstream sensor
& camera takes the picture of incoming chips, then conveyor
reverses direction of travel
 16. WAIT_FOR 1002 OUTPUT 10
Robot acquires the recognized chip
 17. IF 2401
 18.     MOVE_FROM loc_chip TO loc_nominal
Wait until circuit board passes the downstream location
sensor & conveyor reverses direction of travel
 19.     WAIT_FOR 1001 OUTPUT -10
```

```
Robot inserts the acquired chip into socket #1
 20.    MOVE FROM loc_nominal TO loc_socket_1
 21.    IO OUTPUT -12
 22.    IO OUTPUT -2401
Wait until PLCC chip carrying tray reaches upstream sensor
again for the camera to take a picture, then conveyor
reverses direction of travel
 23.    WAIT_FOR 1002 OUTPUT 10
Robot acquires the second recognized chip
 24.    IF 2401
 25.       MOVE FROM loc_chip TO loc_nominal
Wait until the circuit board passes the downstream location
for the second time & conveyor reverses direction of travel
 26.       WAIT_FOR 1001 OUTPUT -10
Robot inserts the second acquired chip into socket #2
 27.       MOVE FROM loc_nominal TO loc_socket_2
 28.       IO OUTPUT -12
 29.       IO OUTPUT -2401
If no chip is found during second chip vision recognition,
abort the operation.
 30.    ELSE
 31.       STOP_ROBOT
 32.    END
If no chip is found during first chip vision recognition,
abort the operation.
 33. ELSE
 34.   STOP_ROBOT
 35. END
End of assembly operation, move the robot to nominal
location and stop the conveyor.
 36. MOVE_TO loc_nominal
 37. IO OUTPUT -11
 38. IO OUTPUT -9
 39. WAIT_UNTIL -9 OUTPUT -2001
```